Studies on the Construction of Artificial Antibody Light Chain, Light and Heavy Chain Fittings and Antigen-Antibody Interactions

July 2019

Hanbing XUE

Studies on the Construction of Artificial Antibody Light Chain, Light and Heavy Chain Fittings and Antigen-Antibody Interactions

A Dissertation Submitted to
the Graduate School of Life and Environmental Sciences,
the University of Tsukuba
in Partial Fulfillment of the Requirements
for the Degree of Doctor of Philosophy in Science
(Doctoral Program in Biological Sciences)

Hanbing XUE

Table of Contents

Abbreviations

Arg: arginine

BSA: bovine serum albumin

CDR: complementarity determining region

CGG: chicken γ-globulin

IgH: immunoglobulin heavy chain

IgL: immunoglobulin light chain

μHC: μ heavy chain

NGS: next generation sequencing

NP: 4-hydroxy-3-nitrophenyl acetyl

NPA: 2-(4-hydroxy-3-nitrophenyl) acetic acid

pre-BCR: pre-B cell receptor

SDS-PAGE: sodium dodecyl sulfate polyacrylamide gel electrophoresis

SLC: surrogate light chain

Abstract

Immunity is one of homeostatic mechanisms of the living body, which can exclude the foreign things different from oneself. In vertebrate, the immune system is divided into innate immunity and acquired immunity. Protection of body with the innate immune system is nonspecific and provides comprehensive responses to pathogens; on the other hand, the acquired immune system causes a stronger and specific immune response, which discriminates and memorizes foreign antigens. Both innate and acquired immunity depend on the ability of immune system to distinguish between self and non-self molecules.

Immunoglobulins play important roles in antigen recognition during the acquired immune response, and the complementarity-determining region (CDR) 3 of the heavy chain is considered as the critical antigen-binding site. There are enormous complexities in the antigen recognition of antibody repertoire, which hampered the explicit understanding of antibody system. Previously a statistical protocol for the extensive analysis of heavy chain variable region repertoires and the dynamics of their immune response using next-generation sequencing (NGS) was developed. In addition, the properties of important antibody heavy chains predicted *in silico* by the protocol were

examined by gene synthesis and antibody protein expression; however, the corresponding light chain that matches with the heavy chain could not be predicted by our protocol. To understand the dynamics of heavy chain and light chain pairing, I firstly tried to obtain an artificial light chain that pairs with a broad range of heavy chains and then analyzed its effect on the antigen binding of heavy chains upon pairing.

During the pre-B cell stage, the surrogate light chain (SLC) could pair with the nascent immunoglobulin μ heavy chains (Ig-μH) and promote them to function in the periphery. On the basis of this property, I designed several versions of genetically engineered “common light chain” prototypes by modifying the SLC structure. Among them, the mouse-derived VpreB1λ5Cκ light chain showed acceptable matching property with several different heavy chains without losing specificity of the original heavy chains, though the antigen affinities were variable. I found that the extent of matching depended on the heavy chain; the conventional IgLs, Vκ_2ORB and Vκ_2A6I, considerably maintained the antigen binding of IGHV9-3 heavy chain but not of IGHV1-72 heavy chain. Thus, the antigen recognition of the heavy chain is variably affected by the paired light chain, and that the artificial light chain, Mm_VpreB1λ5Cκ,

maintained the antigen binding of either heavy chain, indicating its potential to be a "common light chain". These results provide an initiative observation on the correlation of antibody heavy and light chain structures, and also provide a novel system to analyze the effects of light chains pairing in antigen recognition of heavy chains.

General Introduction

The immune system is a mechanism that protects living organisms from disease by identifying and killing abnormal substances such as pathogens and cancer cells in the body. This mechanism can sense a variety of pathogens and distinguish pathogens from their own healthy cells and tissues in order to function properly.

In vertebrate, the immune system includes innate immunity and acquired immunity. Innate immunity does not respond to various pathogens separately but always in “a state of war”, so the time to activate the efficacy is short. Acquired immunity is achieved by cellular immunity of functional cells such as lymphocytes, and humoral immunity of blood proteins such as antibodies and complement. Lymphocytes include T cells and B cells. B cells can differentiate and mature to produce immunoglobulins. In addition, dendritic cells that take up and degrade antigens by phagocytosis and present antigens to T cells are also involved in immune functions. These cells are transported to bone marrow and interact with lymphoid tissues such as the thymus, lymph nodes and spleen to function effectively (Alberts et al., 2002).

Antibody, also known as immunoglobulin, contains four heterologous polypeptide chains. The two chains with larger molecular weight are called heavy chain, and the two

chains with smaller molecular weight are called light chain. The amino acid composition of two H chains and two L chains in the same Ig molecule is identical (Janeway et al., 2001).

The structure of antibodies consists of variable regions and constant regions. The variable regions play important roles in antigen recognition. The variable regions of immuoglobulin heavy chains (IgHs) show enormous diversity by V-D-J gene rearrangements that include random nucleotide additions in the complementarity-determining region (CDR) 3 (Tonegawa, 1983; Xu, Davis et al., 2000). The variable regions of immunoglobulin light chains (IgLs) are less diverse than IgHs because of the lack of D_L gene segments and poor nucleotide insertions (Jackson et al., 2013).

The use of next-generation sequencing (NGS) to analyze antibody repertoires is advantageous for rapid and extensive identification of antigen-specific antibodies (DeKosky et al., 2015; Georgiou et al., 2006; Weinstein et al., 2009). Previously a method for the holistic analysis of IgH and IgL repertoires respectively from mice and humans was reported (Kono et al., 2017; Sun et al., 2019). In contrast to the recent

single cell-based NGS repertoire analysis (Marcus et al., 2006; Dash et al., 2011), this method has an advantage of easy and inexpensive handling of huge numbers of IgH and IgL sequences, but has a disadvantage of inability to determine the pairing of IgH and IgL.

In addition, I developed an intelligible method for detecting antigen-responding IgH repertoires by analyzing dynamic changes in whole antibodies in individual mice during 4-hydroxy-3-nitrophenyl acetyl (NP) hapten and chicken γ-globulin (CGG) antigen immunization and found that the major responding IgHs were IGHV1-72/IGHD1-1/IGHJ2 for NP-hapten and IGHV9-3/IGHD3-1/IGHJ2 for CGG-carrier protein. The former antigen-antibody interaction was extensively analyzed by the crystallography (Mizutani et al., 1995), whereas the latter interaction was a new finding. I confirmed the latter interaction by gene synthesis of NGS reads and antibody protein expression followed by ELISA test. During the course of the study, I realized the lack of information on the mode of interaction between IgH and IgL, and the effect of IgL pairing on the antigen binding affinity of IgH.

In this report, I described examples of IgH/IgL matching in terms of the antigen

binding of IgHs specific to NP-hapten and CGG-carrier antigens. In addition, we attempted the construction of “common light chain” models that preserve the potential to associate with a wide variety of IgHs.

During the early stage of B cell development, the V-D-J rearranged μH pairs with the surrogate light chains (SLCs), VpreB and λ5, to form the pre-B cell receptor (pre-BCR) (Tsubata et al., 1990; Karasuyama et al., 1990). Pre-BCR serves as an important checkpoint and participates in IgH repertoire selection, which is crucial for B cell maturation and migration to the periphery (Mårtensson et al., 2010; Melchers 2015; Sun et al., 2018). These findings suggest that the SLC can bind to various IgHs and select them to function in the peripheral immune system (Boekel et al., 1997). Based on this, I utilized SLC molecules to construct “common light chain” models, and examined their matching ability to various IgHs and their effect on antigen binding affinities of IgHs in comparison to those of conventional IgL. These results would provide useful information on antigen recognition of IgH/IgL pairs and on the optimization of antibody drugs.

Chapter 1

Construction of VpreBλ5Cκ light chains as “common light chain” models

Introduction

To recognize and resist the different kinds of pathogens, antibody diversity is very important. A huge number of about 10^{15} different antibodies can be produced after immunization. This diversity comes from the gene rearrangements, N and P genes insertion, inherent mutagenesis and combination of IgH and IgL.

The CDR3 of IgH is variable and is considered as the most critical antigen-binding site. It has been estimated that the gene rearrangement can result in up to a huge diversity of more than 10^{10} different variations of CDR-H3. It's a "black box" so far. Recently, the advent of NGS methods made it possible to analyze the diversity.

Previously a method for holistic analysis of the immunoglobulin heavy chain (IgH) and light chain (IgL) repertoires respectively from mouse was reported, but it did not determine the pairing of IgH and IgL sequences in that study (Kono, Sun et al. 2017). Comprehensive analysis of heavy chain repertoire by next generation sequencing (NGS) was established as follows. Mice were immunized with antigens. After 2 weeks, the spleen was collected and cDNA of antibody IgHs was used as the template, the universal adapter was ligated to 5' end as the forward primer, and at the 3' end, the

sequences of IgH constant region1 were used as the reverse primer. After sequencing, the heavy chain variable region gene sequences (about 100 k reads) could be obtained. This method has an advantage in easy and inexpensive handling of huge numbers of IgH or IgL sequences but has a disadvantage of inability to determine the pairing of IgH and IgL.

The whole antibody repertoire could be visualized using the three dimensional plots of VDJ genes with 110 IGHV genes, 12 IGHD genes, and 4 IGHJ genes. Thus, It became possible to comprehensively analyze the antibody repertoire in individuals (Kono et al., 2017).

During the antibody expression, secreted nascent heavy chain has to combine with a light chain in the endoplasmic reticulum before detachment from the heavy chain-binding protein (Bole et al., 1986). Therefore, for the expression of the antigen-specific heavy chains detected, analysis of the paired IgH/IgL repertoires has great significance.

Previously, research has been conducted on detection of the natural pairing of antibodies (Meijer et al., 2006). In recent years, using single-cell genome sequencing

(Marcus et al., 2006; Dash et al., 2011), emulsion-based technology was developed for in-depth analysis of paired VH-VL repertoires in large numbers of B cells (>2×10^6 per experiment) (DeKosky et al., 2015). In addition, a frequency-based pairing algorithm for T cell receptor (TCR) pairing was obtained, which accounts for allelic inclusion and sequencing errors (Lee et al., 2017). The light chains (TCRα) have relatively low genetic diversity and might be shared to more than one heavy chain (TCRβ) (Lee et al., 2017; Jackson et al., 2012; Hoi et al., 2013). Thus, these methods might be required for further screening for the most matching IgH/IgL (TCRα/ TCRβ) pairs.

During the early stages of B cell development, rearranged μH pairing with the surrogate light chain (SLC), consisting of VpreB and λ5, forms the pre-B cell receptor (pre-BCR) (Tsubata and Reth, 1990; Karasuyama et al., 1990). Pre-BCR serves as an important checkpoint and the SLC participates in IgH repertoire selection, which is crucial for B cell survival (Mårtensson et al., 2010; Melchers, 2015; Sun et al., 2018). These findings suggest that the SLC can bind to various matured heavy chains expressed on the B cell surface.

Previous research on paired heavy- and light-chain antibody repertoires has shown

that the public CDR-L3 genes generally have low frequency of nucleotide insertions at VJ junctions, which are closer to the germ line. SLCs do not have nucleotide insertions and lack mutations, consistent with the characteristics of common light chains (DeKosky et al., 2015). In addition, the similar CDR regions in conventional light chain sequences can also be found in the SLC sequences (Ohnishi and Melchers, 2003).

In the current study, using the SLC sequences, I constructed a "common light chain" to resolve the issues regarding the antigen-specific heavy chains lacking matching light chains detected in our previous study and provided a new approach for analyzing the pairing of light and heavy chains.

Materials and Methods

Construction of VpreBλ5Cκ light chains

On the basis of the SLC structures, the engineered VpreBλ5Cκ light chains were constructed by the following processes: 1. the "tail" domain of λ5 was cut; 2. the redundant non-Ig part of VpreB was cut and removed; 3. the terminal of VpreB and the "tail" of λ5 were spliced to form a new CDR-L3 loop; 4. the Arg101Tyr mutation was introduced into VpreB; 5. the engineered VpreB-λ5 light chain variable region (VpreBλ5) was connected to the human Igκ constant region (Cκ) already present in the antibody expression vector (Mammalian PowerExpress System, TOYOBO MPH-101).

Cell culture

Before and after transfection, CHO-S cells were maintained in Dulbecco's Modified Eagle's Medium (D-MEM, Wako) medium supplemented with 10% fetal bovine serum (Cell Culture Biosciences), 1% MEM Non-Essential Amino Acids, 1% Pen Strep, 2 mM L-glutamine, and 1 mM sodium pyruvate (all from GIBCO) and rested in a humidified 37°C incubator.

DNA plasmids and antibody gene syntheses

The synthesized genes in the pTAKN vector (Eurofins) were inserted into an antibody-expression vector (Mammalian Power Express System, TOYOBO) containing the human-derived Igγ1 heavy chain constant region gene and the Igκ light chain constant region gene. All the DNA plasmids were expanded in TOP10 Chemically Competent *Escherichia coli* (Invitrogen) and purified with the QIAprep Spin Miniprep or Midi/Maxprep Kit (Qiagen) according to the manufacturer's instructions.

The heavy-chain variable region genes synthesized were inserted into the pEHgammaX1.1 (TOYOBO) vector using the BsiWI and NheI sites. The light-chain variable genes synthesized were inserted into the pELkappaX2.2 (TOYOBO) vector using the BsiWI and MluII sites. The heavy chain and light chain expression vectors were ligated with the Quick Ligase Kit (New England BioLabs) to construct intact antibody expression vectors.

Transfection and antibody protein expression

5 μL of DNA (0.5 μg/mL) and 6.25 μL Lipofectamine LTX (Invitrogen) were incubated in 500 μL Opti-MEM I Reduced Serum Medium (GIBCO). After incubation for 25 min at room temperature (25°C), all of the medium was added to the pre-prepared 6-well cell culture dishes containing about 70% CHO-S cells in 2 mL of CHO medium lacking penicillin-streptomycin and incubated for 4 h at 37°C. Then, the antibiotic-free medium was changed to the medium containing penicillin-streptomycin and incubated at 37°C overnight. After 24 h, 20 μg/mL puromycin was added for cell selection. The stably transfected cell colony was obtained approximately 7 days later, and the supernatant was collected after 2 weeks.

Immunoassays

The antibody concentration of the supernatant samples was adjusted to the same level as follows. Ninety-six well Maxisorp Nunc-Immuno plates (Thermo) were coated with unconjugated anti-human IgG polyclonal antibody (Dako) at 1:500 dilution in coating buffer (50 mM sodium carbonate-bicarbonate buffer, pH 9.6) and incubated at 4°C overnight. Then, 1% bovine serum albumin (BSA, Sigma) in phosphate-buffered saline

(PBS, Sigma) was used for blocking at room temperature (RT, 25°C) for 1 h. Standard curves were constructed using a purified influenza-specific human IgG recombinant antibody (National Institute of Infectious Diseases, Japan) at serial dilutions ranging from 12.5 to 800 ng/mL in wash buffer (PBS containing 0.05% Tween-20) at RT for 2 h. Then, the plates were further incubated with horseradish peroxidase (HRP)-conjugated anti-human IgG antibody (Dako) at RT for 1 h. Color development was performed with o-Phenylenediamine dihydrochloride (OPD, Sigma) buffer (0.05 M citrate-PO_4 buffer, pH 5.0) containing 0.4 mg/mL OPD and 0.04% v/v 30% H_2O_2. The absorbance was measured at 490 nm. When the concentration of the reference was between 25 and 400 ng/mL (50 and 800 ng/mL), a linear relationship was obtained between absorbance and concentration in the fitted curve, with $R^2 > 0.97$.

To determine the binding capacity of antibody samples (Fig. 10, Fig. 16B and Fig. 17), the supernatants were diluted in wash buffer, and the antibody concentration was adjusted to 10 μg/mL. NP-BSA and CGG antigens were coated in coating buffer at a concentration of 10 μg/mL and incubated at 4°C overnight. After blocking, cell culture supernatants were added to each well. After 1 h of incubation at RT, the plates were

incubated with HRP-conjugated anti-human IgG (H+L) antibody (Jackson ImmunoResearch) at 25°C for 1 h. The binding activities of the antibodies are expressed in terms of O.D. 450 nm.

***In silico* simulation**

All the steps for homology modeling and ligand docking were performed using the Molecular Operating Environment (MOE) software. The crystal structure of the conventional light chain (PDB: 1NGP) was chosen as the template for homology modeling. The intermediate structures were obtained by induced-fit homology modeling using the reaction-field electrostatics and the Amber12: EHT force field parameters, which are suitable for both protein and small molecules (AmberTools 12 Reference Manual, 2015; Hoffmann, 1963). The generalized Born/volume integral (GB/VI) method was used for the model scoring (Labute, 2008). The protonation was performed before refining the final model by using Protonate3D in the MOE software (Labute, 2014). The final models were further refined by gradient minimization until the RMS gradient was lower than 0.05 kcal mol^{-1} $Å^{-1}$.

The final models were docked with the NPA molecule from the crystal structure (1NGP) in Protein Data Bank using default settings. Briefly, the Triangle Matcher was used for placement, the Rigid Receptor was used for refinement, the London dG was used for initial scoring, and the GBVI/WSA dG was used for final scoring (Gentile et al., 2015).

The final structures were checked with PROCHECK (Laskowski et al., 1993), and the interaction patterns between receptors and ligands were analyzed with the MOE software. The residue scans were also performed for the heat stability analysis of the mutations using MOE.

Gene classification

Phylogenetic tree was used for gene classification. The tree was generated using the neighbor-joining (NJ) algorithm with the MEGA7 software by analyzing the protein sequences.

Statistical analysis

Statistical analysis was performed in Microsoft Excel. The error bars on the figures indicate the standard deviation from the mean. Student's *t*-test was used to evaluate the significances of differences between experimental data.

Results

Concept of the "common light chain"

The rearrangement of IgH genes occurs before that of IgL genes, where the surrogate light chain (SLC) is associated with nascent IgH instead of IgL (Fig. 1). Here, sequence alignments were performed between SLC (the sequences from PDB: 2H32) and conventional λ1 light chain (the sequence from PDB: 3PIQ). The region similar to CDR3 in the SLC was composed of a portion of VpreB and λ5 close to the non-Ig region (Ohnishi and Melchers, 2003) (Fig. 2). As shown in Fig. 3, I modified the different SLCs to form the VpreBλ5 light chains. Based on the SLC structures, the engineered VpreBλ5Cκ light chains were constructed by the following processes: 1. Cut the "tail" domain of λ5; 2. Cut and remove the redundant non-Ig part of VpreB; 3. Splice the terminal of VpreB and the "tail" of λ5 to form a new CDR-L3 loop; 4. Introduce the mutation of Arg101Tyr in VpreB; 5. Connect the engineered VpreB-λ5 light chain variable region (VpreBλ5) to the human Igκ constant region (Cκ) that was already present in the antibody expression vector.

Difference between species of SLC sequences

Different VpreB and λ5 genes from different species were compared and classified (Fig. 4 and Fig. 5). The sequence similarity and identity were analyzed. The regions corresponding to CDR-L3 in VpreB and λ5 showed the significant differences. Because the SLC gene sequences differ among various species, both human and mouse-derived VpreB1λ5 light chains (Hs_VpreB1λ5 and Mm_VpreB1λ5) were designed (Fig. 4). It showed that VpreB1 and VpreB2 sequences were quite similar, however VpreB3 sequences were different. At an early phase of assembly, Ig-μH also associates with VpreB3 and λ5 (Shimizu et al., 2002, Ohnishi and Takemori, 1994). I compared the gene sequences between human-derived VpreB1 and VpreB3 and synthesized the Hs_VpreB3λ5 light chain gene (Fig. 5).

Construction of antigen-antibody complex *in silico*

In order to assess the antigen bindings of NP-specific IgHs paired with each light chain models (Mm_λ1Cκ, Mm_VpreB1λ5Cκ, and Hs_VpreB1λ5Cκ), *in silico* docking simulations were performed. The crystal structure 1NGP was as the control, which is

the original structure of IGHV1-72/Mm_λ1 antibody. Through the comparison of protein sequences of IgHs and IgLs from different antibodies, I found that the similarity of IgHs and IgLs compared to the sequences from 1NGP were more than 30% (Fig. 6A). Thus, the 1NGP structure was used as the template for homology modeling and the final structures were evaluated using Ramachandran plot (Phi-Psi plot), more than 98% residues fall within the allowed ranges (Fig. 6B). The antigen-antibody complexes containing the small molecule antigen (NP) were constructed using docking simulation.

Effect of the Arg in the middle of the CDR-L3

In the previous studies, the most significant IgH repertoires were found to be NP-specific IGHV1-72 (short for IGHV1-72/IGHD1-1/IGHJ2) and CGG-specific IGHV9-3 (short for IGHV9-3/IGHD1-1/IGHJ2) (Kono, Sun et al. 2017). To make it consistent with the λ1 light chain already known to pair with IGHV1-72 (Mizutani et al., 1995), the positively charged arginine (Arg) in the middle of the new CDR-L3 of VpreB1λ5Cκ was replaced with a tyrosine (Tyr) carrying no charge (R101Y, RtY) (Fig. 3 and Fig. 4). Upon introducing *in silico* mutations of R101Y in Mm_VpreB1λ5Cκ and

Hs_VpreB1λ5Cκ, I found that the Arg residues in the middle of CDR-L3 in both Mm_VpreB1λ5Cκ and Hs_VpreB1λ5Cκ decreased the affinity for 4-hydroxy-3-nitrophenylacetic acid (NPA) when paired with IGHV1-72Cγ (Fig. 7A); the replacement of Arg with Tyr also appeared to affect the heat stability of paired complexes (Fig. 7B).

Effects on the substitution of human-derived C_{κ} for $C_{\lambda 5}$

The originally designed VpreB1λ5 light chains were connected to a human-derived Igκ constant region (Fig. 3). I also tested binding capacity after the replacement of the human-derived Igκ constant region with the human-derived Igλ5 constant region by ELISA test (Fig. 8). The concentration of the antibody in cell culture supernatant was adjusted to the same. Standard curves were constructed using a purified influenza-specific human IgG recombinant antibody at serial dilutions. When the concentration of the reference was between 25 and 400 ng/mL (50 and 800 ng/mL), a linear relationship was obtained between absorbance and concentration in the fitted curve, with $R^2 > 0.97$ (Fig. 9A); the acceptable recoveries were shown in different

concentrations (Fig. 9B). The antibody capacities were significantly reduced by the replacement with λ5 constant region (Fig. 10), which were consistent with the results of NPA-binding *in silico* (Fig. 11). Thus, human-derived Igκ constant region was used in all of my "common light chain" models.

Discussion

I modified the SLC structures to attempt to design the "common light chains" (VpreBλ5Cκ), which might be able to pair with broad-spectrum antigen-specific heavy chains detected by the formerly reported method.

Previously, the mice were immunized with NP-CGG and CGG antigens, and the NP- and CGG- specific IgH gene repertoires were exhaustively analyzed using NGS (Kono et al., 2017), to address the lack of information regarding paired light chains, I focused on the maturation process of B-cell receptors in the early stage of B cell development. Theoretically, the SLC would most likely exist as a "common light chain" to different heavy chains. The structures of the SLC show remarkable homology with the conventional light chain (Ohnishi and Melchers, 2003), the SLC could be transformed into a structure similar to the conventional light chain.

The similar work focusing on variable domain of the modified SLC has been successfully performed (Morstadt et al., 2008). Further, for the study on pairing of IgH and IgL, the recombinant light chains from different species and isotypes were synthesized, which were linked to a human Igκ constant region for expressing an intact

light chain. I aimed to design a light chain with extensive matching to the heavy chains and maintain the antigen specificity and affinity after matching.

By classification analysis using protein sequences, it was found that the VpreB1 and VpreB2 sequences were similar, however VpreB3 sequences were quite different. Initially, to analyze the antigen binding, I constructed all three VpreB1λ5 light chains (Mm_VpreB1λ5, Hs_VpreB1λ5 and Hs_VpreB3λ5) *in silico*. In fact, because the former constructed two human-derived VpreB1λ5 seemed fail to maintain the binding capacity of IGHV1-72, especially the Hs_VpreB3λ5 lost more binding affinity of both IGHV1-72 and IGHV9-3. After this, I constructed the mouse-derived VpreB1λ5 light chain.

Because the positively charged Arg(+) was frequently found in CDR3 of poly-reactive (auto-reactive) antibodies and it does not exist in the original λ1 light chain. Here, to analyze the possible effects of the positively charged Arg on antigen binding, Arg was replaced by the uncharged Tyr. The effect of the mutation of Arg to Tyr (RtY) in CDR-L3 on antigen binding was discussed by *in silico* simulation. After docking for NP binding, I found that the Args in the middle of CDR-L3 in both

Mm_VpreB1λ5Cκ and Hs_VpreB1λ5Cκ decreased the affinity for NP when paired with IGHV1-72Cγ. The residue scan showed that the RtY mutation also appeared to improve the thermal stability of paired complexes. So the RtY mutation was introduced into the "common light chain" models.

The variable domain of the antibody is significant in antigen recognition. In recent years, the effects of light chain constant regions on antibody expression and antigen binding have been studied (Lee et al., 1999; Janda et al., 2016). The effect of JC regions of λ5 or κ on heavy chain maturation and cell surface expression in pre-B cell lines was researched, the result showed that the mouse-derived λ5 JC region and κ JC region were used to co-express with several types of HC and JC λ5 promotes heavy chain maturation and expression more significantly compared to JC κ (Smith and Roman, 2010). However, the effect on the antigen affinity of heavy chain was not yet known. In this study, I compared the effects of the Igκ constant region and Igλ5 constant region on antigen binding for NP and CGG. Significant differences were noted in some cases in antigen binding. I continued to use the original Igκ given by the expression vector in my models.

Further, all the constructed antibodies consisting of the SLC-modified light chain and the mouse-derived antigen specific heavy chain were examined for antigen binding capacities to confirm the conception of “common light chain”.

Chapter 2

Pairing of constructed light chain models to IgHs and their effect on antigen recognition of IgHs

Introduction

During B cell development, the rearrangement of IgH genes occurs before that of IgL genes, where the surrogate light chain (SLC) is associated with nascent IgH in place of IgL, and as reported before, approximately 50% of the newly rearranged heavy chains can bind to surrogate light chain at the pre-B stage and differentiate into mature B cells (Boekel et al., 1997). The variable domains of antibody heavy chains show rich diversity and are encoded by three different loci, that is, the variable (V), diversity (D), and joining (J) gene segments (Tonegawa, 1983). Nucleotide addition in the complementarity-determining region (CDR) 3 hypervariable region provides additional diversity for antigen recognition and binding (Xu et al., 2000). The light chain variable region (V_L) is less diverse than those of the heavy chain variable region (V_H) because of the lack of D gene segments (Jackson et al., 2013). Besides, by the comparison of SLC and conventional light chain sequences, it was found that the similar CDR regions of conventional light chain also existed in SLC (Ohnishi and Melchers, 2003). Thus, the surrogate light chain might have a propensity to be modified to the conventional light chain and be associated with a wide range of IgHs.

In the previous study, NGS method was used to analyze the antigen-specific antibody responses. The specific IgH repertoires were determined by the common antibody repertoire in immunized 5 mice. In the Naïve mice group, there was no antigen-responding antibody repertoire detected. In NP-CGG and CGG immunized mice groups, it was found that the major responding IgHs were IGHV1-72 for NP-hapten and IGHV9-3 for CGG-carrier protein. IGHV1-72 is the well-known NP-responding antibody and the detected CGG-responding IGHV9-3 is the new finding. The antigen specificities were confirmed by gene synthesis of NGS reads. *In silico* analysis of antigen-specific antibody was done to confirm their antigen specificities initially, then the antibody protein expression experiments were performed.

In the constructed antibodies, all of the constant regions are given by the expression vectors. The λ1 variable domain is known as the original pair of IGHV1-72. Because the IgH/IgL pairing could not be predicted by the protocol, so the λ1 variable domain was also used to pair with IGHV9-3 for confirming the CGG specificity. After stable expression, the cell culture supernatants were collected and examined for antigen specificity. As the result shown, when only CGG was as the antigen, IGHV1-72

antibody did not react as expected, and IGHV9-3 antibody reacted with CGG in a low but significant reactivity. It was confirmed that IGHV9-3 is actually the CGG specific heavy chain. However, compared to the reactivity of IGHV1-72 to NP, the reactivity of IGHV9-3 to CGG was very low. Here, I thought that the pairing of IgH and lgL was improper and had impact on the antigen binding. The following work, I focus on the analysis of IgH/IgL pairing.

In this study, I constructed the engineered "common light chain" (VpreBλ5Cκ) models from two species. In order to examine the matching to IgHs, firstly, the constructed light chains were paired with two representative IgHs (NP-specific IGHV1-72 and CGG-specific IGHV9-3). In addition, the conventional IgLs were also constructed as controls. The expression and secretion of paired IgH/IgL complex was confirmed by Western Blot of the culture supernatant. My results suggested that the Mm_VpreB1λ5Cκ seemed to have the potential to be the "common light chian".

Besides, the CDR3 region of IgH is usually considered as the most important antigen-binding site. However, in the detected antigen-specific IgH repertoires reported before, it was known that a critical binding site (R50) is located in CDR2 in NP-specific

IGHV1-72 (Mizutani et al., 1995) and considerable CGG-specific IGHV9-3 repertoires containing the same variable region and different diversity and joining regions (Kono et al., 2017). Here, I also examined the possible antigen-binding site in both these two IgHs and analyzed the binding patterns by *in silico* simulation and antibody expression experiments. My finding showed that the different effects on the paired IgLs between small antigen binding (NP hapten) and protein antigen binding (CGG carrier).

The purposes of my study were as follows. 1. Understanding of the dynamics of IgH/IgL pairing. 2. Analysis of the effect of IgL pairing on antigen binding of IgH. As far as I know, there is no research on these questions. 3. Construction of the artificial light chain that pairs with a broad range of heavy chains. It means to search for the "common light chain".

Materials and Methods

Cell culture

This was performed as described in Chapter 1.

DNA plasmids and antibody gene synthesis

This was performed as described in Chapter 1.

Transfection and antibody protein expression

This was performed as described in Chapter 1.

Immunoassays

This was performed as described in Chapter 1.

To determine the binding affinity of the antibodies (Fig. 19), the serial diluted concentration of antibody samples and the constant concentration of antigens (5 μg/mL) were used. The steps for the ELISA were the same as those described above.

Western blot analysis

Antibody expression in the supernatant was analyzed by western blotting. The antibodies from the supernatant were separated using 12% SDS-PAGE and electroblotted onto 0.45-μm nitrocellulose membranes (Bio-Rad). Then, 5% skim milk in wash buffer (50 mM Tris-HCl, pH 7.5, 0.1 M NaCl, 0.05% v/v Tween-20) was used for blocking at 4°C overnight. The immunoblot was treated with HRP-conjugated goat anti-human IgG (H+L) antibody (Jackson ImmunoResearch) (Fig. 12) or HRP-conjugated goat anti-human IgG (Dako) and HRP-conjugated goat anti-human Igκ (SouternBiotech) (Fig. 21) at 1:5000 dilution. SuperSignal West Femto (Pierce) was used as the substrate for chemiluminescence.

***In silico* simulation**

This was performed as described in Chapter 1.

After docking, all the complexes were refined by a short MD simulation for 5 ns in NAMD (https://www.ks.uiuc.edu/Research/namd/) with the Amber12: EHT force field and R-field solvation. The protocol was as follows: all the complexes were put into a

water box with periodic boundary conditions and the margin was set to 10Å; energy minimization for the whole system was performed by applying gradient minimization until the RMS gradient fell below 0.05 kcal mol^{-1} $Å^{-1}$; heating for 10 ps from 0 K to 310 K; equilibration for 10 ps at 310 K; production phases for 5 ns at 310 K. The stable conformations were analyzed for NPA-binding.

Statistical analysis

This was performed as described in Chapter 1.

Results

Pairing of constructed light chain models to IGHV1-72 and IGHV9-3

The synthesized genes in the pTAKN vector were inserted into an antibody-expression vector (Mammalian Power Express System, Toyobo) containing the human-derived Igγ1 heavy chain constant region gene and the Igκ light chain constant region gene. The expression and secretion of paired IgH/IgL complexes were confirmed by western blot of culture supernatants, showing that all light chain models (Mm_VpreB1λ5Cκ, Hs_VpreB1λ5Cκ, and Hs_VpreB3λ5Cκ) were paired with IGHV1-72Cγ and IGHV9-3Cγ heavy chains (Fig. 12).

Interaction patterns between receptor and ligand in IGHV1-72 antibodies

To assess the stereo-chemical qualities and antigen bindings of NP-specific IgHs paired with each light chain model (Mm_λ1Cκ, Mm_VpreB1λ5Cκ, and Hs_VpreB1λ5Cκ). The crystal structure 1NGP was as the control, which is the original structure of IGHV1-72/Mm_λ1 antibody. *In silico* docking simulations were performed, after 5ns molecular dynamic simulation, the optimized conformations were evaluated

using Procheck (Fig. 13). The optimal antigen binding patterns were analyzed. The structures of 1NGP and IGHV1-72Cγ/Mm_λ1Cκ have the same antibody variable domains and antigen. The interaction of the IGHV1-72Cγ/Mm_λ1Cκ complex was similar with the crystal structure (1NGP). The NP-specific IGHV1-72Cγ paired with Mm_λ1Cκ, Mm_VpreB1λ5Cκ, and Hs_VpreB1λ5Cκ showed the conserved antigen-binding site Arg50 in all three antibodies; however, Arg50 was found to bind to different oxygen molecules in IGHV1-72Cγ/Mm_λ1Cκ (Fig. 14).

Prediction of the antigen-binding sites in IGHV9-3

The dominant CGG-specific IgH repertoires include the same V_H (IGHV9-3) and different D_H and J_H regions (Fig. 15), suggesting that the antigen specificity was not exerted by CDR-H3. To test the involvement of CDR-H1 and CDR-H2 in antigen binding, several mutations were introduced into CDR-H1 and -H2 (Fig. 16A). As shown in Fig. 14, Arg50 of IGHV1-72 was predicted to be one of the major residues to interact with NP. Consistently, the R50A mutant remarkably lost its antigen binding affinity (Fig. 16B). Similarly, all mutations in CDR-H1 and CDR-H2 of IGHV9-3

significantly induced a loss of binding affinities, suggesting that these regions were involved in the binding to CGG (Fig. 16B).

Comparison of binding capacities among the "common light chain" candidates *in silico*

In order to predict the antigen binding capacities of NP-specific IgHs paired with each light chain models (Mm_VpreB1λ5Cκ, Hs_VpreB1λ5Cκ), the docking simulations were performed. The binding energies as the docking result were compared. I used both general models and induced-fit models to do the docking simulation with NPA. The results of general models are in accordance with those of induced-fit models. In addition, comparing the docking results and the ELISA test, it showed that the predicted results and the detected results are generally consistent (Fig. 7 and Fig. 17). The Mm_VpreB1λ5Cκ showed higher binding energy than Hs_VpreB1λ5Cκ, though compared to the original light chain (Mm_λ1), the binding energy is lower (Fig. 7).

Mm_VpreB1λ5Cκ maintained the binding capacities of IGHV1-72 and IGHV9-3

Among the light chain models constructed, Mm_VpreB1λ5Cκ properly maintained the binding of IGHV1-72 to NP antigen, although its binding capacity with the original light chain (Mm_λ1Cκ) was significantly higher. In addition, Mm_VpreB1λ5Cκ also maintained a high binding capacity of IGHV9-3 to CGG, whereas pairing with Mm_λ1Cκ decreased the binding capacity remarkably (Fig. 17). Hs_VpreB1λ5Cκ showed significant non-specific binding to NP-BSA, when paired with IGHV9-3 (Fig. 17). I also compared the non-specific binding to NP-BSA between Mm_VpreB1λ5Cκ and Hs_VpreB1λ5Cκ *in silico,* when paired with IGHV9-3 (Fig. 18). The result showed a higher binding energy, when IGHV9-3 paired with Hs_VpreB1λ5Cκ, which is consistent with the ELISA test.

Mm_VpreB1λ5Cκ maintained the binding affinities of IGHV1-72 and IGHV9-3

I also detected the antigen binding by serial dilution of antibody concentration. In the NP-BSA binding test, the NP antigen was recognized at the concentration of 0.8 μg/mL when IGHV1-72 paired with Mm_VpreB1λ5Cκ and Mm_λ1Cκ, however it was recognized by other antibodies at higher concentrations; In the CGG-binding test, the

CGG antigen was recognized at the concentration of 0.2 μg/mL when IGHV9-3 paired with Mm_VpreB1λ5Cκ, while it was recognized at higher concentration when IGHV9-3 paired with Mm_λ1Cκ (Fig. 19). These results suggested that Mm_VpreB1λ5Cκ had the ability to pair with either IGHV1-72 or IGHV9-3 maintaining the antigen recognitions of IgHs.

Differences between the binding pattern of small molecule antigen (NP hapten) and protein antigen (CGG carrier)

It is noteworthy that conventional IgLs, Vκ_2ORB and Vκ_2A6I, considerably maintained the antigen binding of IGHV9-3 but not that of IGHV1-72 (Fig. 17 and Fig. 19), suggesting that the significant differences on the conventional IgLs pairing with different IgHs. Combined the results above together. It suggested that the protein antigen (CGG) binding to IGHV9-3 antibodies is less affected by the IgL; the NP hapten as small molecule binding to the IGHV1-72 antibodies is significantly affected by IgLs. These results showed the differences between the binding pattern of small molecule antigen and protein antigen.

Discussion

I modified the SLC structures to construct three “common light chain” candidates. It was found that the chimeric genetic engineering antibody consisting of a mouse-derived variable region and a human-derived Igκ constant region could pair with both of heavy chains (IGHV1-72 and IGHV9-3) without losing the heavy chain antigen specificity and could maintain the affinity derived from heavy chains to a certain extent.

I did the *in silico* analysis of the binding pattern of constructed antibodies to NP antigen. In order to analyze the interaction between antibody and antigen, the crystal structure 1NGP was as the control, which is the original structure of IGHV1-72/Mm_λ1 antibodies and the other three models were also constructed. *in silico* docking simulations were performed and the optimal antigen binding poses were analyzed. In these three constructed structures, the conserved antigen-binding site Arg50 was shown; however Arg50s were found bound to different oxygen molecules in IGHV1-72Cγ/Mm_λ1Cκ, suggesting that the change of paired light chains might result in the broken of the original hydrogen bond. It implies that the binding pattern of IGHV1-72 to NP is affected by paired IgLs.

All the light chains tested matched with IGHV9-3 and maintained the reactivity to CGG. V9-3 combined several different diversity (D) and joining (J) regions to form different IGHV9-3 antibodies. In the variable domain, CDR1 and CDR2 are only encoded by the V region, whereas CDR3 includes a portion of the V regions and all of the D and part of the J regions (Xu and Davis, 2000). Taken together, these findings suggest that the main domain of antigen recognition in IGHV9-3 might be more likely to be located on CDR1 and CDR2. I also confirmed the effect of several amino acids in CDR1 and CDR3 of IGHV9-3 on binding affinity. Although the effect of different light chains on CDR-H1 and CDR-H2 is not known, this is probably the reason why IGHV9-3 maintained its reactivity to CGG after matching with different light chains.

All the antibodies of the human-derived light chain that bound to the mouse-derived heavy chain had low affinities for NP-BSA. This might be related to the differences between species. Depending on the distance between residues on the V_H-V_L interface, the antibodies were divided into three different clusters. Two representative light chains were chosen as the control to pair with both IGHV1-72 and IGHV9-3: the human-derived cluster A light chain (PDB: 2ORB.L) and mouse-derived cluster B light

chain (PBD: 2A6I.L). Mouse antibodies include a part of Cluster A and Cluster B, whereas human antibodies all belong to Cluster A (Chailyan et al., 2011). It implies that the mouse-derived light chains might have wider compatibility than the human-derived light chains.

According to these results, it showed the significant differences between two conventional IgLs when paired with different IgHs. The two conventional IgLs (2ORB.L and 2A6I.L) preserved the antigen binding affinity of IGHV9-3, suggesting that the surface to surface wide interaction between antigen and antibody (CGG and IGHV9-3 antibody) is less affected by the conformation skew brought by the IgLs. However, the two conventional IgLs failed to preserve the antigen binding affinity of IGHV1-72. NP hapten as small molecule binds to IGHV1-72 antibodies, the mode of antigen binding (IGHV1-72 antibody to NP) would be “lock and key” mode, thus prone to the conformation skewing by IgLs. It might elucidate that why the Mm_VpreB1λ5Cκ maintained the binding capacity of IGHV1-72 but Hs_VpreB1λ5Cκ did not, while both two VpreB1λ5Cκ maintained the binding capacity of IGHV9-3 to CGG.

The current findings, together with our previous study involving the use of NGS for

exhaustive analysis of antibody repertoires, provide a new approach for recognizing antigen-specific antibodies and the pairing of heavy and light chains and also aid in the artificial expression of important antigen-specific heavy chains for which data on paired light chains are not available.

Chapter 3

Mm_VpreB1λ5Cκ can pair with several IgHs

Introduction

To confirm the antigen specificity of the IgH repertoires detected, I attempted to express the related antibodies *in vitro* by using gene synthesis technology. However, after immunization, a wide variety of light chain repertoires were produced and the corresponding light chain that would be well matched with the heavy chain repertoires detected could not be predicted by our method. My aim was to find a "common light chain" to pair with a broad range of heavy chains.

Based on the property of SLC, I designed several versions of genetically engineered "common light chain" prototypes by modifying the SLC structure. Among them the Mm_VpreB1λ5Cκ light chain showed acceptable matching property with two different heavy chains (IGHV1-72 and IGHV9-3) without losing specificity from the original heavy chains.

Further, I detected the matching of Mm_VpreB1λ5Cκ and more antigen-specific IgHs. Another three IgHs were chosen as NP-specific and CGG-specific IgH repertoires, respectively. Using artificial antibody expression, I examined the matching and antigen-binding capacity of the light chain designed to the different heavy chain

samples. The mouse-derived VpreBλ5 light chain showed a good match with several different heavy chains without losing specificity to the original heavy chains. Thus, the results suggest that engineered light chains could effectively help solve the issues related to the expression of the antigen-specific heavy chains detected by NGS and are of significance in vaccine development.

In this study, I used the mouse-derived IgHs as the heavy chain models to examine the matching of both mouse- and human-derived VpreBλ5 IgLs. Although the mouse- and human-derived IgHs keep the genetic similarities to some extent, the current results showed that the human-derived IgL could not well pair with mouse-derived IgHs. I thought that the "common light chain" probably should be considered in different species. To test my hypothesis, I used the Mm_VpreB1λ5Cκ and Hs_VpreB1λ5Cκ to pair with three reported IgHs from different families of human and mouse. The constructed antigen-antibody complexes from mouse and human were performed with 5 and 10 ns molecular dynamic simulation using Amber14, respectively. The binding energies were calculated after the conformation kept stable with MMPBSA method. The results showed that all the VpreBλ5 light chain antibodies maintained certain

binding capacity to corresponding antigens, compared to the original antibody structures.

In conclusion, based on the property of SLC, the genetically engineered VpreBλ5 light chains by modifying the SLC structure might have the potential to be the "common light chain".

Materials and Methods

Cell culture

This was performed as described in Chapter 1.

DNA plasmids and antibody gene synthesis

This was performed as described in Chapter 1.

Transfection and antibody protein expression

This was performed as described in Chapter 1.

Immunoassays

This was performed as described in Chapter 1.

In Fig. 22, cell culture supernatants were incubated with antigens (5 μg/mL) pre-coated in microtiter plate wells. The other steps were the same as those described above. The binding activities of the antibodies are expressed in terms of O.D. 490 nm.

Western blot analysis

This was performed as described in Chapter 1.

Gene classification

This was performed as described in Chapter 1.

Statistical analysis

This was performed as described in Chapter 1.

***In silico* simulation**

This was performed as described in Chapter 1.

The final models were docked with peptides from the crystal structures (shown in Fig. 23) in Protein Data Bank using Protein-Protein Docking in MOE.

After docking, the molecular dynamics simulations were performed in Amber with the ff14SB force field. The protocol was as follows: all the complexes were put into a 10Å water box with periodic boundary conditions; initially, energy minimization for water and ions was performed with 1000 steps of conjugate gradient methods; energy

minimization for all atoms was performed using 200 steps of steepest descent method, followed by 4800 steps of conjugate gradient method; heating for 10 ps from 0 K to 310 K; equilibration for 10 ps at 310 K under 1 atmosphere conditions; production phases at 310 K. The stable conformations were analyzed for binding energy using MM/PBSA method in Amber16 software (Srinivasan, Cheatham et al. 1998; Kollman, Massoya et al. 2000).

Results

Mm_VpreB1λ5Cκ can pair with several IgHs

To examine the ability of Mm_VpreB1λ5Cκ to match with different heavy chains, three additional NP-specific IgHs (IGHV1-53/D1-1/J2, IGHV6-3/D1-1/J2, and IGHV14-3/D1-1/J2) and three CGG-specific IgHs (IGHV1-69/D1-1/J2, IGHV1-55/D1-1/J3, and IGHV1-52/D2-4/J2) were chosen and then we tested the preservation of antigen binding of each IgH (Fig. 20). These chosen antigen-specific IgH repertoires were classified. Phylogenetic tree was generated using the neighbor-joining (NJ) algorithm (Fig. 20). It suggested that all these IgHs belong to several families.

Western blot analysis of the cell culture supernatants confirmed the expression and secretion of all antibodies. The molecular weight (~55 kDa) of the heavy chains and the different molecular weights (~25 kDa) of the light chain (Mm_VpreB1λ5Cκ) were observed (Fig. 21), suggesting that all the chosen IgHs paired with Mm_VpreB1λ5Cκ and all the antibodies were secreted out of the cell successfully.

All the examined antibodies significantly bound to the corresponding original

antigens maintaining the specificity and affinity and showed significantly greater binding capacity than the negative control (CHO medium), suggesting that Mm_VpreB1λ5Cκ is able to pair with a wide variety of IgHs maintaining their antigen specificities (Fig. 22).

***In silico* simulation of Mm_VpreB1λ5Cκ and Hs_VpreB1λ5Cκ pairing with IgHs from different clans**

IgHs derived from different clans, were chosen as samples for testing the binding capacity, including the mouse-derived IgH sequences from the reported structures (PDB ID): 1A3R, 5EOQ and 2HRP (Fig. 23A) (Torom et al., 1994; Kaever et al., 2016; Lescar et al., 1997); the human-derived IgH sequences from the reported structures (PDB ID): 5ERW, 3MOD and 4XMK (Fig. 23B) (Kachko et al., 2015; Yang et al., 2013; Kumar et al., 2015).

Induced-fit homology modeling was used to construct the VpreB1λ5Cκ antibody. The binding energies were calculated preliminarily from the docking result. The small RMSD values between the co-crystallized and the docked ligands were shown and it

proved that the docking structure were good (Fig. 24). The Plots for the calculated binding energies between the original structures and VpreB1λ5Cκ antibody structures were shown as docking score (Fig. 25), the similar binding energy suggested that the VpreB1λ5Cκ light chain can pair with the corresponding IgHs and maintain the binding affinity of IgHs.

5ns molecular dynamics simulation was performed for mouse-derived antibody complex and 10ns molecular dynamics simulation was performed for human-derived antibody complex (Fig. 26 and Fig. 27). The trajectories from the stable conformations were chosen for the calculation of binding energy with MM/PBSA method. The binding energies between the original and VpreB1λ5Cκ structures were compared (Fig. 28), and the results suggested that Mm_VpreB1λ5Cκ and Hs_VpreB1λ5Cκ might pair with IgHs from different clans maintaining their specificities.

Discussion

I designed an engineered light chain, which can associate with several different heavy chains from mouse antibodies. The IgHs from several families detected before were utilized to pair with mouse-derived VpreB1λ5 to determine the matching of IgH and IgL. These data imply that the Mm_VpreB1λ5 light chain showed a good match with several different heavy chains without losing specificity of the original heavy chains. However, the study has some limitations, such as limited samples and low affinities. On the one hand, the low affinity might be caused by the original binding capacity from IgHs. On the other hand, it might because the affect of paired IgL. In further studies, I plan to work on the matching of heavy chains from different species and to further improve binding affinity after matching through genetic modification on VpreBλ5 light chains.

In addition, I considered the "common light chain" in different species and analyzed the mouse- and human-derived VpreB1λ5Cκ light chain pairing with the reported IgHs from corresponding species. *In silico* simulation showed that, comparing with the original structures, mouse- and human-derived VpreB1λ5Cκ were well-matched with

heavy chains from different clans and maintained the antigen binding capacity of the original antibodies to some extent. Although the experimental data is still in simulation stage.

In summary, Mm_VpreB1λ5Cκ, has the potential to be a “common light chain”, providing a novel system to dissect the mode of IgH/IgL interaction and contributing a new seed for antibody drug development. Mm_VpreB1λ5Cκ could be used as a standard light chain, which can associate with wide varieties of IgHs, and it would be possible to examine the properties of IgHs without the bias of inherent light chains. It could be as a novel tool to investigate the IgH/IgL interaction dynamics.

General Discussion

In this study, I ascertained that the chimeric antibody consisting of a mouse-derived SLC variable region and a human-derived Igκ constant region could pair with several IgHs without losing the IgH antigen specificity and could maintain the antigen affinity of IgHs to a certain extent.

Previously NP- and CGG- specific IgH repertoires and their dynamics on a whole were analyzed using NGS, and utilized the gene synthesis and expression system for the evaluation of important antibodies; however, the antigen binding seemed significantly affected by the chosen IgL (Kono et al., 2017). I thought that if the antigen binding of both IgH and IgL can be separately analyzed, it would provide a novel experimental system to dissect the antigen binding dynamics of an antibody. I hypothesized that if the standard IgL, which can associate with a wide variety of IgH can be used, it would be possible to examine the molecular properties of IgHs without the bias of various inherent light chains. For the model of IgH/IgL pairing, it was reported that some IgLs can be shared by more than one IgH because IgL is less diverse than IgH (Jackson et al., 2012; Hoi and Ippolito, 2013).

The SLC would most likely exist as a “common light chain” for different IgHs

because peripheral B cells use SLC for their IgH counterparts during their early development in the bone marrow (Karasuyama et al., 1990; Mårtensson et al., 2010; Melchers, 2015). Because the structures of the SLC remarkably show homology with the conventional IgL (Ohnishi and Melchers, 2003), I tried to transform the SLC molecules to construct "common light chain" models. A similar work focusing on the variable domain of SLC has been reported, but the ability to pair with IgHs was not evaluated (Morstadt et al., 2008).

The Mm_VpreB1λ5Cκ molecule is associated with NP-specific IGHV1-72 IgH and CGG-specific IGHV9-3 IgH maintaining the antigen specificities and abilities, whereas Hs_VpreB1λ5Cκ and Hs_VpreB3λ5Cκ showed incomplete maintenance of antigen specificities. I tested the replacement of Cκ with $C_{\lambda 5}$ but the antigen binding properties were not improved.

It was reported that, depending on the distances and interactions between residues on the V_H-V_L interface, antibodies can be classified into three different clusters (Mouse antibodies are grouped into both Cluster A and Cluster B, whereas human antibodies all belong to Cluster A) (Chailyan et al., 2011). This implies that some mouse-derived IgLs

might have wider heavy chain compatibility than human-derived IgLs. Two representative lgLs were chosen as the control to pair with both IGHV1-72 and IGHV9-3: the human-derived cluster A IgL (PDB: 2ORB.L) and mouse-derived cluster B IgL (PBD: 2A6I.L). Surprisingly, the conventional IgLs, mouse 2A6I.L and human 2ORB.L, preserved the antigen binding affinity of IGHV9-3; however, these conventional IgLs failed to preserve the antigen affinity of IGHV1-72, suggesting significant differences in these IgH properties. IGHV9-3 used various IGHD genes in binding to CGG antigen, suggesting that the major antigen binding sites is CDR-H1 or CDR-H2. In fact, mutations in CDR-H1 and CDR-H2 impaired CGG binding. I speculate that the wide surface-to-surface interaction of an antigen and an antibody is less affected by the conformation skew induced by IgL species. In contrast, IGHV1-72 mainly used IGHD1-1 for NP-binding, suggesting that the major binding site is CDR-H3 in addition to R50 in CDR-H2. In this case, the mode of antigen binding would be “lock and key” mode, which is prone to conformational skewing by the chosen IgL. In this context, Mm_VpreB1λ5Cκ was able to preserve the antigen recognitions of these distinct IgHs.

In this study, I constructed an engineered “common light chain” prototype, Mm_VpreB1λ5Cκ, which can associate with several IgHs. It would be possible to improve the versatility of Mm_VpreB1λ5Cκ by *in silico* simulations and immunoassays to provide a novel antibody model in which the interference between IgH and IgL is properly controlled and insulated for optimized antigen recognition of artificial antibodies.

Acknowledgments

I gratefully appreciate Prof. Dr. Kazuo Ohnishi (National Institute of Infectious Diseases) for supervision of the course for doctoral degree. I am also thankful to Dr. Lin Sun, Prof. Dr. Hirofumi Fujimoto and Prof. Dr. Yoshimasa Takahashi for helpful advice and comments. I would like to express my gratitude to Ms. Sayuri Yamaguchi for valuable technical assistance.

References

AmberTools 12 Reference Manual. https://ambermd.org/doc12/AmberTools12.pdf (accessed 10 March 2015).

Alberts B., Johnson A., Lewis J. et al., Molecular Biology of the Cell, 4th edition, New York: Garland Science 2002.

Chailyan A., Marcatili P., Tramontano A., The association of heavy and light chain variable domains in antibodies: implications for antigen specificity, FEBS J. 278 (2011) 2858–2866.

DeKosky B.J., Kojima T., Rodin A. et al., In-depth determination and analysis of the human paired heavy- and light-chain antibody repertoire, Nat. Med. 21 (2015) 86–91.

Dash P., McClaren J.L., Oguin 3rd T.H. et al., Paired analysis of TCRα and TCRβ chains at the single-cell level in mice, J. Clin. Invest. 121 (2011) 288–295.

Gentile F., Deriu M.A., Licandro G. et al., Structure Based Modeling of Small Molecules Binding to the TLR7 by Atomistic Level Simulations, Molecules. 20 (2015) 8316–8340.

Georgiou G., Ippolito G.C., Beausang J. et al., The promise and challenge of high-throughput sequencing of the antibody repertoire, Nat. Biotechnol. 32 (2014) 158–168.

Hoffmann R., An Extended Hückel Theory. I. Hydrocarbons. J. Chem. Phys. 39 (1963) 1397.

Hoi K.H., Ippolito G.C., Intrinsic bias and public rearrangements in the human immunoglobulin Vλ light chain repertoire, Genes. Immun. 14 (2013) 271–276.

Janda A., Bowen A., Greenspan N.S. et al., Ig Constant Region Effects on Variable Region Structure and Function, Front. Microbiol. 10 (2016) Article 22.

Jackson K.J.L., Kidd M.J., Wang Y. et al., The shape of the lymphocyte receptor: lessons from the B cell receptor, Front. Immunol. 4 (2013) Article 263.

Janeway J.C.A., Travers P., Walport M. et al., Immunobiology: The Immune System in Health and Disease, 5th edition, New York: Garland Science 2001.

Jackson K.J.L., Wang Y., Gaeta B.A. et al., Divergent human populations show extensive shared IGK rearrangements in peripheral blood B cells, Immunogenetics 64 (2012) 3–14.

Kachko A., Frey S.E., Sirota L. et al., Antibodies to an interfering epitope in hepatitis C virus E2 can mask vaccine-induced neutralizing activity, Hepatology 62 (2015) 1670-1682.

Karasuyama H., Kudo A., Melchers F., The proteins encoded by the VpreB and lambda 5

pre-B cell-specific genes can associate with each other and with mu heavy chain, J. Exp. Med. 172 (1990) 969–972.

Kaever T., Matho M.H., Meng X. et al., Linear Epitopes in Vaccinia Virus A27 Are Targets of Protective Antibodies Induced by Vaccination against Smallpox, 90 (2016) 4334-4345.

Kollman P.A., Massova I., Reyes C. et al., Calculating structures and free energies of complex molecules: combining molecular mechanics and continuum models, Acc. Chem. Res. 33 (2000) 889-897.

Kumar R., Pan R., Upadhyay C. et al., Functional and Structural Characterization of Human V3-Specific Monoclonal Antibody 2424 with Neutralizing Activity against HIV-1 JRFL, J. Virol. 89 (2015) 9090-9102.

Kono N., Sun L., Toh H. et al., Deciphering antigen-responding antibody repertoires by

using next-generation sequencing and confirming them through antibody-gene synthesis, Biochem. Biophys. Res. Commun. 487 (2017) 300–306.

Labute P., Protonate 3D: Assignment of macromolecular protonation state and geometry. http://www.ccl.net/cca/documents/proton/ (accessed 31 March 2014).

Labute P., The generalized Born/volume integral implicit solvent model: Estimation of the free energy of hydration using London dispersion instead of atomic surface area. J. Comput. Chem. 29 (2008) 1693–1698.

Lee Y.K., Brewer J.W., Hellman R. et al., BiP and immunoglobulin light chain cooperate to control the folding of heavy chain and ensure the fidelity of immunoglobulin assembly, Mol. Biol. Cell 10 (1999) 2209-2219.

Laskowski R. A., MacArthur M. W., Moss D. S. et al., PROCHECK: A program to check the stereochemical quality of protein structures, J. Appl. Crystallogr. 26 (1993)

283–291.

Lescar J., Stouracova R., Riottot M.M. et al., Three-dimensional structure of an Fab-peptide complex: structural basis of HIV-1 protease inhibition by a monoclonal antibody, J.Mol.Biol. 267 (1997) 1207-1222.

Melchers F., Checkpoints that control B cell development, J. Clin. Invest. 125 (2015) 2203–2210.

Mårtensson I.-L., Almqvist N., Grimsholm O. et al., The pre-B cell receptor checkpoint, FEBS Lett. 584 (2010) 2572–2579.

Meijer P.J., Andersen P.S., Haahr Hansen M. et al., Isolation of human antibody repertoires with preservation of the natural heavy and light chain pairing, J. Mol. Biol. 358 (2006) 764–772.

Marcus J.S., Anderson W.F., Quake S.R., Microfluidic single-cell mRNA isolation and analysis, Anal. Chem. 78 (2006) 3084–3089.

Morstadt L., Bohm A., Yüksel D. et al., Engineering and characterization of a single chain surrogate light chain variable domain, Protein Sci. 17 (2008) 458–465.

Mizutani R., Miura K., Nakayama T. et al., Three-dimensional structures of the Fab fragment of murine N1G9 antibody from the primary immune response and of its complex with (4-hydroxy-3-nitrophenyl) acetate, J. Mol. Biol. 254 (1995) 208–222.

Ohnishi K., Melchers F., The nonimmunoglobulin portion of lambda5 mediates cell-autonomous pre-B cell receptor signaling, Nat. Immunol. 4 (2003) 849–856.

Ohnishi K., Takemori T., Molecular components and assembly of mu.surrogate light chain complexes in pre-B cell lines, J. Biol. Chem. 269 (1994) 28347–28353.

Srinivasan J., Cheatham T.E., Cieplak P. et al., Continuum solvent studies of the stability of DNA, RNA, and phosphoramidate–DNA helices, J. Am. Chem. Soc. 120 (1998) 9401–9409.

Sun L., Kono N., Shimizu T. et al. Distorted antibody repertoire developed in absence of pre-B cell receptor formation, Biochem. Biophys. Res. Commun. 495 (2018) 1411–1417.

Sun L., Kono N., Toh H. et al., Analysis and visualization of mouse and human antibody repertoires by next-generation sequencing, J. Vis. Exp. 145 (2019) e58804.

Shimizu T., Mundt C., Licence S. et al., VpreB1/VpreB2/λ5 triple-deficient mice show impaired B cell development but functional allelic exclusion of the IgH locus, J. Immunol. 168 (2002) 6286–6293.

Smith B.P. and Roman C.A.J., The unique and immunoglobulin-like regions of surrogate light chain component λ5 differentially interrogate immunoglobulin

heavy-chain structure, Mol. Immunol. 47 (2010) 1195-1206.

Tonegawa S., Somatic generation of antibody diversity, Nature 302 (1983) 575–581.

Tormo J., Blaas D., Parry N.R. et al., Crystal structure of a human rhinovirus neutralizing antibody complexed with a peptide derived from viral capsid protein VP2, EMBO J. 13 (1994) 2247-2256.

Ten Boekel E., Melchers F., Rolink A.G., Changes in the V(H) gene repertoire of developing precursor B lymphocytes in mouse bone marrow mediated by the pre-B cell receptor, Immunity 7 (1997) 357–368.

Tsubata T., Reth M., The products of pre-B cell-specific genes (lambda 5 and VpreB) and the immunoglobulin mu chain form a complex that is transported onto the cell surface, J. Exp. Med. 172 (1990) 973–976.

Weinstein J.A., Jiang N., White III R.A. et al., High-throughput sequencing of the zebrafish antibody repertoire, Science 324 (2009) 807–810.

Xu J.L., Davis M.M., Diversity in the CDR3 region of VH is sufficient for most antibody specificities, Immunity 13 (2000) 37–45.

Yang G., Holl T.M., Liu Y. et al., Identification of autoantigens recognized by the 2F5 and 4E10 broadly neutralizing HIV-1 antibodies, J. Exp. Med. 210 (2013) 2241-2256.

Figures

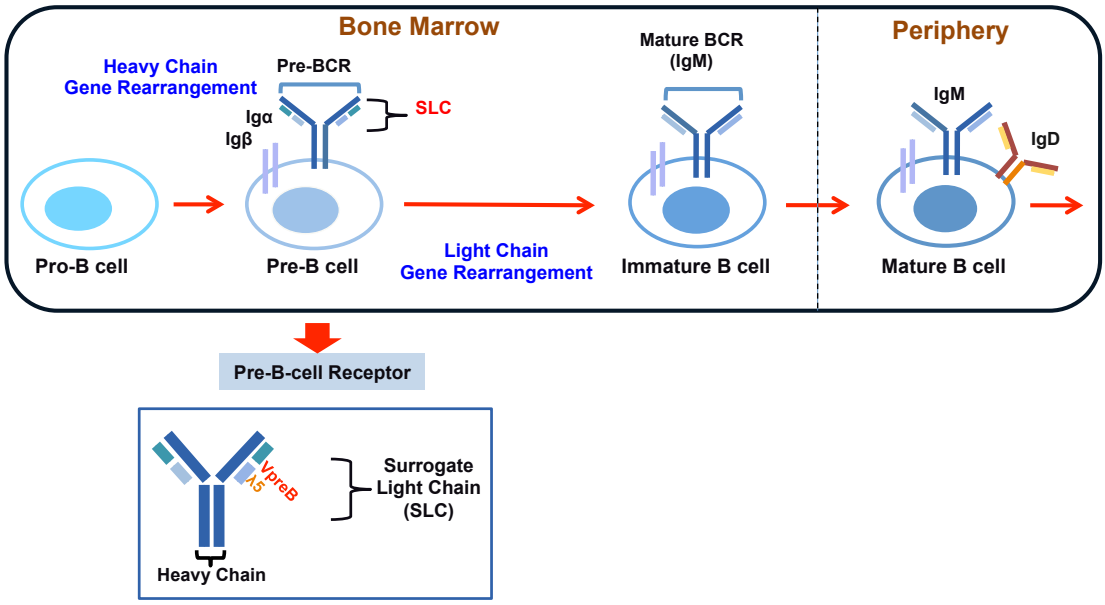

Fig. 1: Concept of the "common light chain". During B cell development, approximately 50% of the newly rearranged heavy chains can bind to the surrogate light chain at the pre-B stage and differentiate into mature B cells. Thus, the surrogate light chain might have a propensity to be the common light chain associating with most of the heavy chains in the periphery.

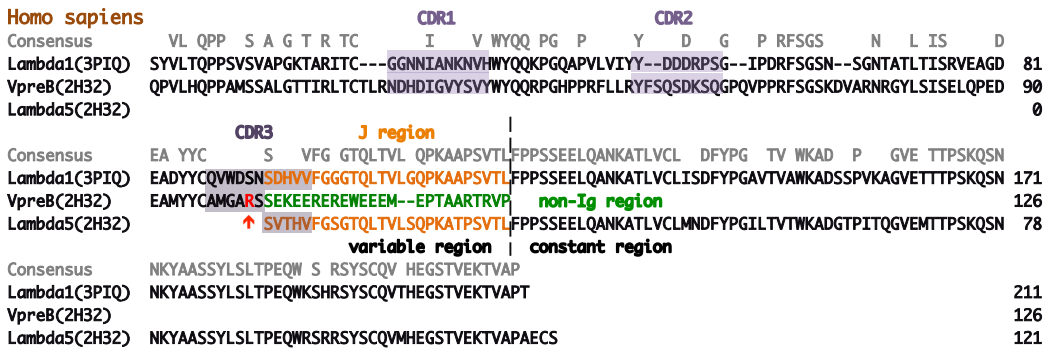

Fig. 2: Comparison between human-derived conventional light chain sequence (PDB: 3PIQ, bottom) and surrogate light chain sequence (PDB: 2H32, top) after alignment. The identical amino acids are indicated at the top of the sequence. Non-Ig region, J region, and CDR3 are annotated in green, orange, and purple, respectively. The red arrow indicates the positively charged Arg in the middle of VpreB (PDB: 2H32).

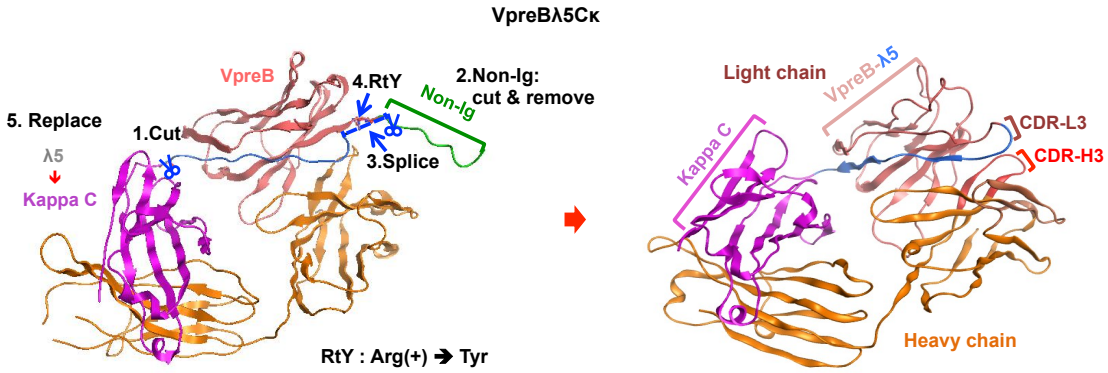

Fig. 3: Construction of recombinant VpreBλ5Cκ light chains. Structural map of the genetically engineered light chain. VpreB (red), Cκ (purple), and heavy chain (orange) are shown. The "tail" of λ5 is highlighted in blue, and the non-Ig domain of VpreB is highlighted in green. The mutation from Arg to Tyr in CDR-L3 was annotated. The steps involved in genetic modification (left) are labeled in appropriate order: 1. Cut the "tail" of λ5; 2. Cut and remove the non-Ig region of VpreB; 3. Splice the "tail" of λ5 to VpreB; 4. Introduce the mutation of Arg101Tyr into VpreB; 5. Replace the λ5 with the human-derived Cκ. The intact antibody Fab (right) is also shown. In addition, all the variable regions of IgHs were connected with the human derived Igγ constant region as described in Materials and Methods.

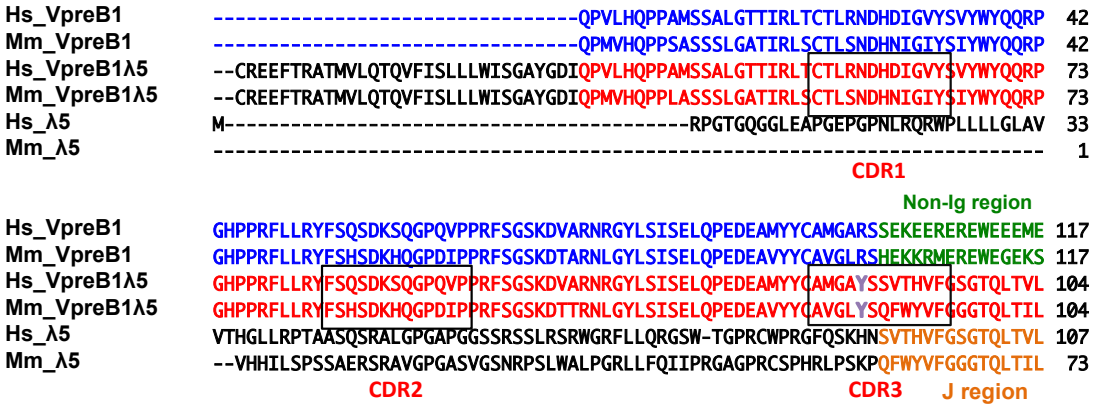

Fig. 4: Alignment of the partial amino acid sequences of VpreB1 and λ5 compared to that of those of VpreB1λ5 constructs derived from humans and mice. The variable regions of VpreB1λ5 and the corresponding regions in VpreB1 and λ5 are indicated in red, blue, and orange, respectively. The non-Ig region in VpreB is indicated in green. The mutation of Arg to Tyr is also highlighted in purple. The CDR regions in VpreB1λ5 constructs are annotated using the Kabat numbering scheme.

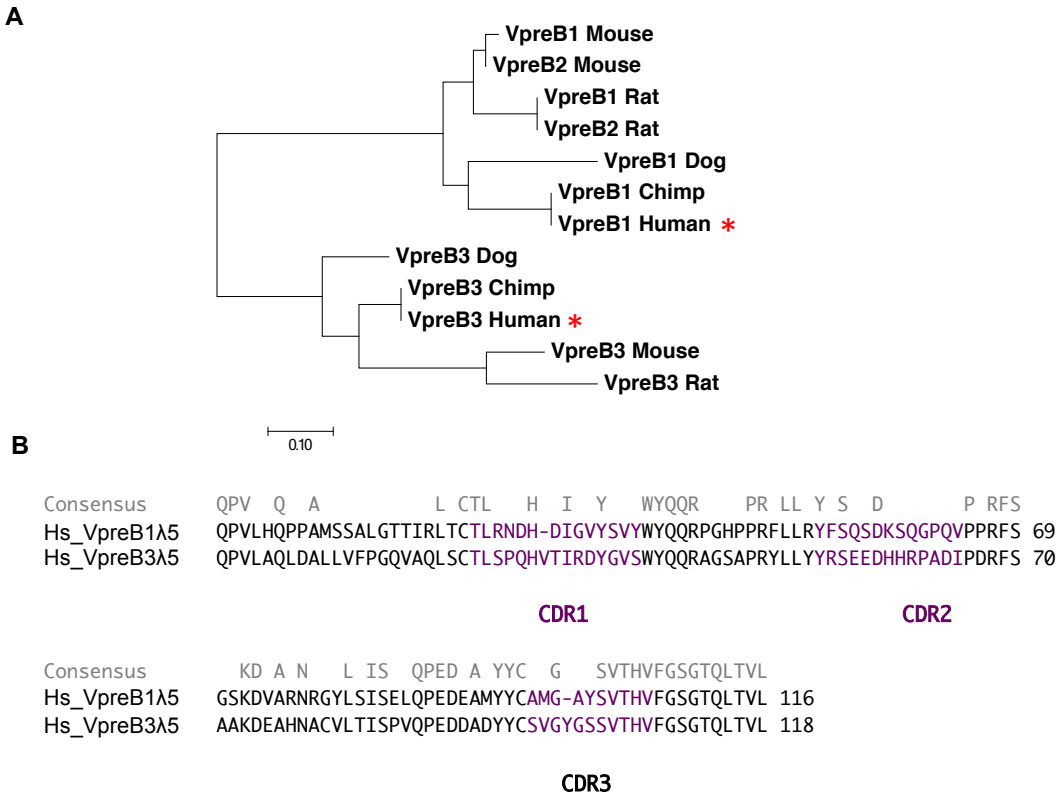

Fig. 5: Construction of Hs_VpreB3λ5. (A) Phylogenetic tree for different VpreB genes from several species. The tree was generated using the neighbor-joining (NJ) algorithm with the MEGA7 software. (B) Comparison between Hs_VpreB1λ5 and Hs_VpreB3λ5 sequences. The CDRs are annotated in purple.

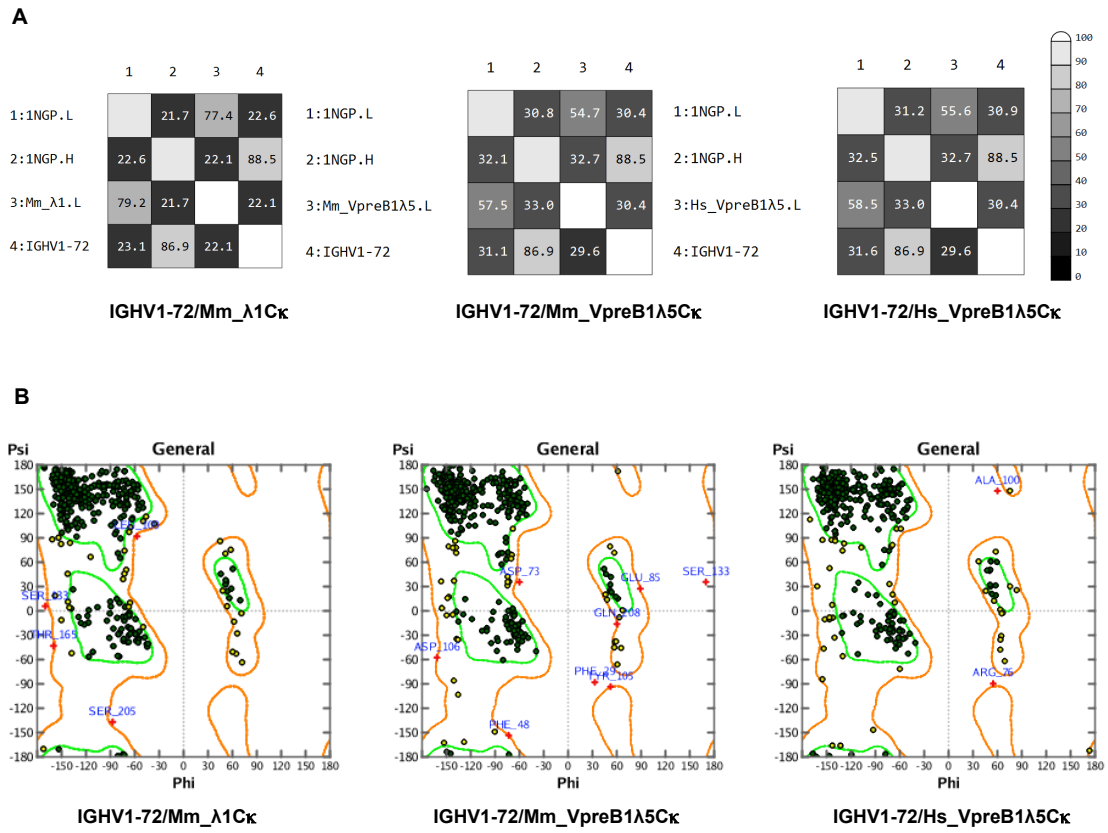

Fig. 6: Homology modeling for the "common light chain" antibodies. (A) The similarity between the template (the sequences from 1NGP) and the constructed antibodies are shown: IGHV1-72Cγ/Mm_λ1Cκ (left), IGHV1-72Cγ/Mm_VpreBλ5Cκ (middle), IGHV1-72Cγ/Hs_VpreBλ5Cκ (right). (B) Ramachandran plot for evaluating the constructed antibody structures. IGHV1-72Cγ/Mm_λ1Cκ (left), IGHV1-72Cγ/Mm_VpreBλ5Cκ (middle), IGHV1-72Cγ/Hs_VpreBλ5Cκ (right).

A

Docking for NPA binding

Antibody	Docking score (kcal/mol)	ΔEnergy (kcal/mol)
IGHV1-72/Mm_λ1Cκ	-7.3216	
IGHV1-72/Mm_VpreBλ5Cκ_Ori	-6.3627	0.0000
IGHV1-72/Mm_VpreBλ5Cκ_RtY	-6.7815	-0.4188
IGHV1-72/Hs_VpreBλ5Cκ_Ori	-6.1419	0.0000
IGHV1-72/Hs_VpreBλ5Cκ_RtY	-6.2030	-0.0611

B

Residue Scan
IGHV1-72/Mm_VpreBλ5Cκ-NPA complex

Mutation	Stability(kcal/mol)	ΔStability(kcal/mol)
R101R	-18.9144	0.0000
R101Y	-20.5613	-1.6469

Residue Scan
IGHV1-72/Hs_VpreBλ5Cκ-NPA complex

Mutation	Stability(kcal/mol)	ΔStability(kcal/mol)
R101R	-18.7342	0.0000
R101Y	-20.2467	-1.5125

Fig. 7: The effects of the mutations from Arg to Try in CDR3 of VpreBλ5Cκ light chains. (A) Docking for NPA binding. IGHV1-72/Mm_λ1 serves as the reference. Docking score (free energy of binding) are shown. (B) Residue scan performed for R101 in the antibody-antigen complex: IGHV1-72Cγ/Mm_VpreBλ5Cκ (left) and IGHV1-72Cγ/Hs_VpreBλ5Cκ (right). The mutation R101Y causing the increase in stability is highlighted in red.

Human kappa constant region

RTVAAPSVFIFPPSDEQLKSGTASVVCLLNNFYPREAKVQWKVDNALQSGNSQESVTEQDSKDSTYSLSSTLTLSKADYEKHKVYA
CEVTHQGLSSPVTKSFNRGEC

Human lambda5 constant region

RTKATPSVTLFPPSSEELQANKATLVCLMNDFYPGILTVTWKADGT-PITQGVEMTTPSKQSNNKYAASSYLSLTPEQWRSRRSYS
CQVMHEG--STVEKTVAPAEC

Fig. 8: Comparison between human kappa constant region and human lambda5 constant region. The replacement of the human-derived Igκ constant region with the human-derived Igλ5 constant region was performed.

A

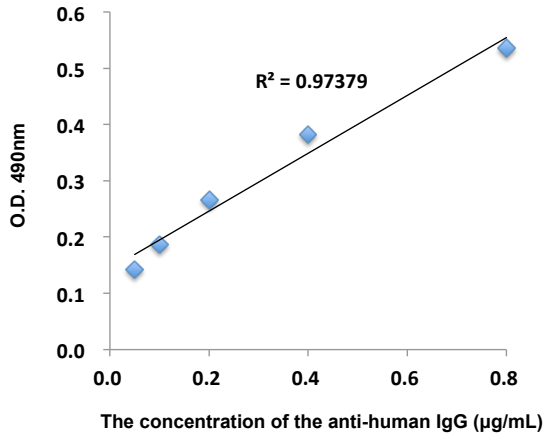

B

Theoretical value (μg/mL)	Test value (mean, n=3, μg/mL)	Recoveries (%)
0.100	0.085	85 ± 4.5767
0.200	0.239	120 ± 2.4831
0.400	0.465	93 ± 3.9964
0.800	0.763	95 ± 2.7981

Fig. 9: A representative curve fitting for concentration measurement. (A) When the concentration of the reference was between 50 and 800 ng/mL, a linear relationship was obtained between absorbance and concentration in the fitted curve, with $R^2 > 0.97$. (B) The recoveries were calculated with the theoretical value and test value.

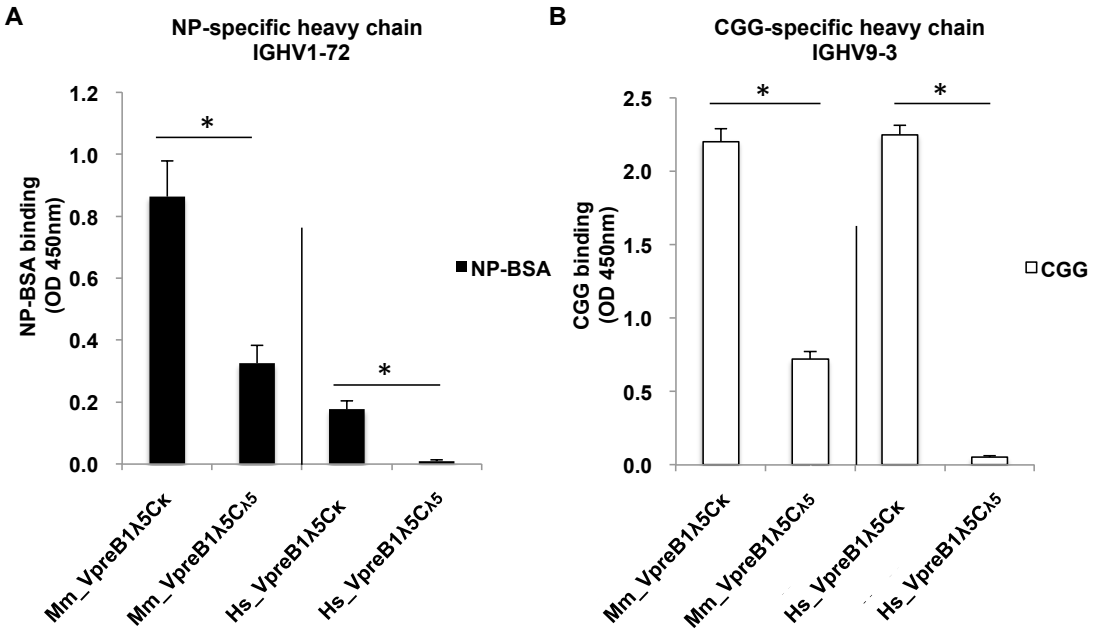

Fig. 10: Antigen binding capacity after the replacement of the human-derived Igκ constant region with a human-derived Igλ5 constant region. (A) ELISA analysis of NP antigen binding capacity of IGHV1-72 antibodies. (B) ELISA analysis of CGG antigen binding capacity of IGHV9-3 antibodies. Statistical significance was tested using Student's *t*-test (*; $P<0.05$, $n = 3$).

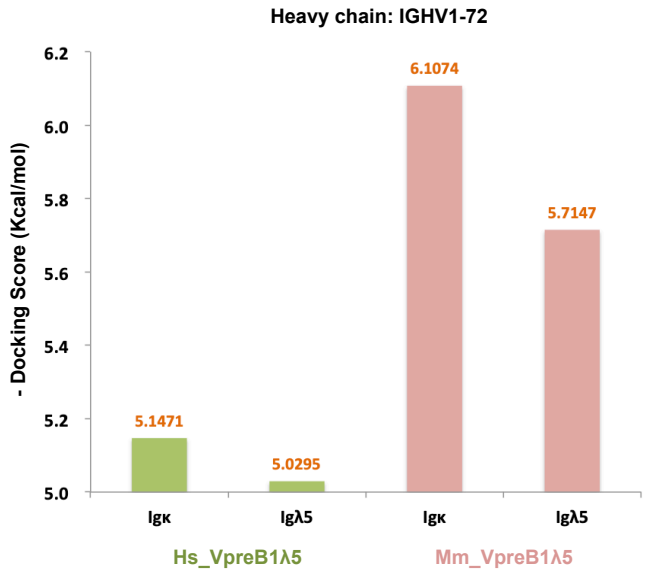

Fig. 11: Docking simulation results for human-derived Igκ and Igλ5 constant region antibodies binding to NPA molecule. The results are shown as - docking scores (binding energy).

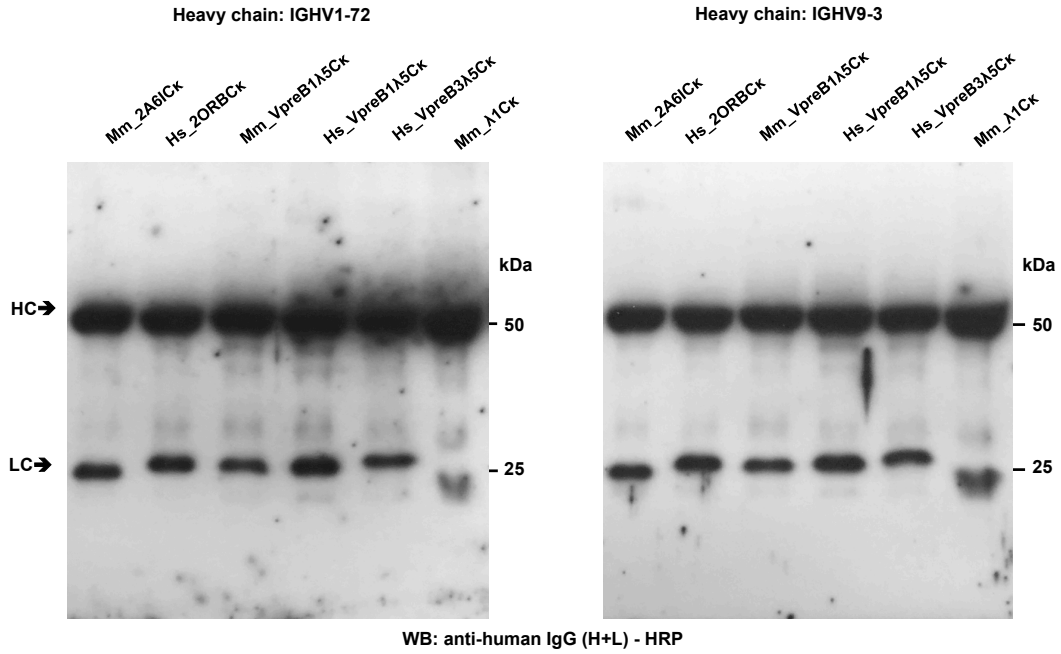

Fig. 12: Matching of different light chains and mouse-derived NP- and CGG-specific heavy chains. Western blot analysis was used for detecting the expression of recombinant antibodies. The heavy chain (top) and light chain (bottom) bands are shown.

	Procheck Evaluation of the stereo-chemical quality of a protein structure			
Structure	Core	Additional	Generously	Disallowed
1NGP	85.5%	12.8%	1.1%	0.6%
IGHV1-72Cγ/Mm_λ1Cκ	83.3%	14.8%	1.1%	0.8%
IGHV1-72Cγ/Mm_VpreBλ5Cκ	80.7%	16.9%	0.8%	1.6%
IGHV1-72Cγ/Hs_VpreBλ5Cκ	80.7%	18.2%	0.5%	0.5%

Fig. 13: Prediction of binding pattern between receptors and ligand *in silico.* Evaluation of the crystal structure of NP-specific 1NGP antibody, and the structure of the antibody models containing NP-specific IGHV1-72 and three different light chains after refinement. The percentage of residues in most favoured, additional allowed, generously allowed and disallowed regions in Ramachandran Plot are shown.

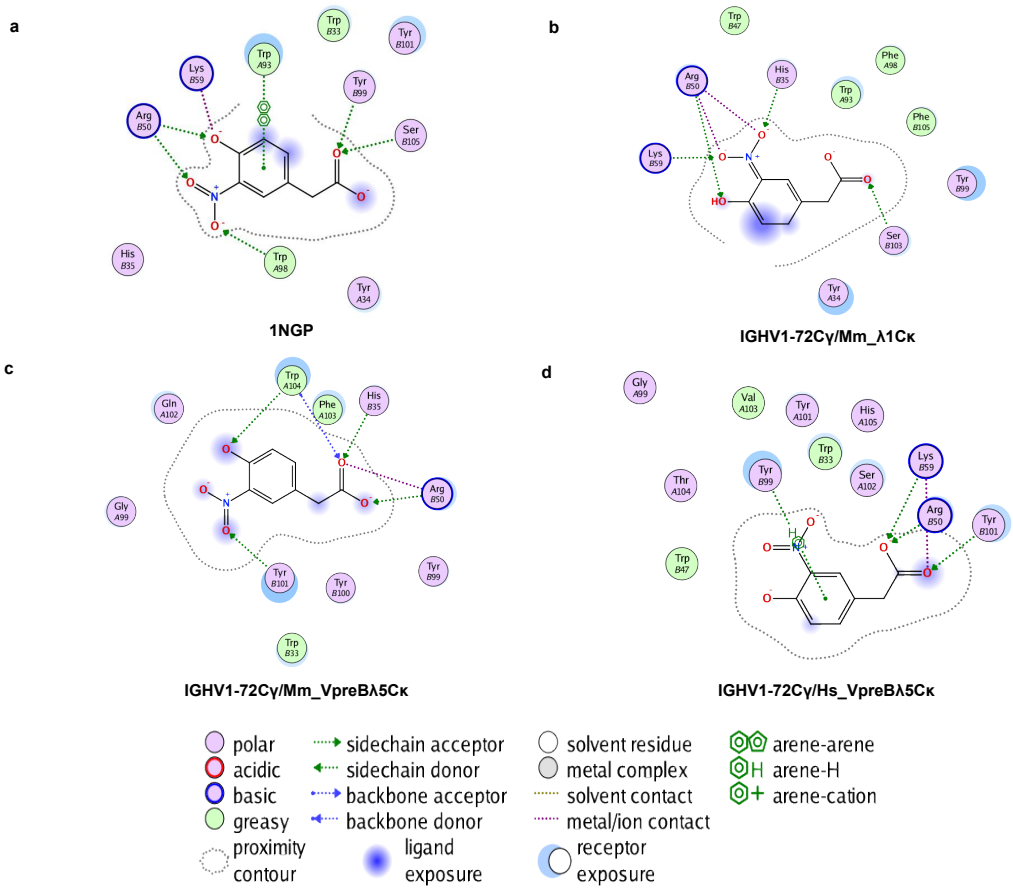

Fig. 14: Interactions between NPA and different receptors. (a) Binding pose of crystallographic structure of 1NGP; (b) Optimal binding pose between NPA and IGHV1-72/Mm_λ1; (c) Binding pose for IGHV1-72/Mm_VpreBλ5; (d) Binding pose for IGHV1-72/Hs_VpreBλ5.

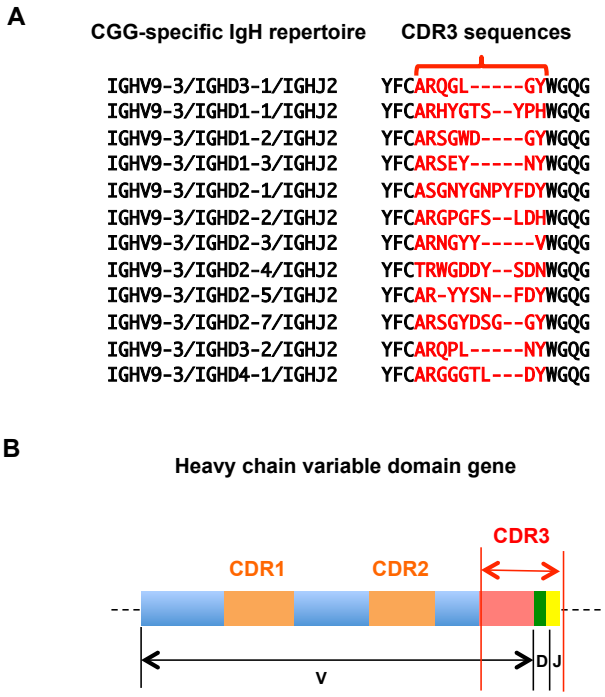

Fig. 15: The genetic organization of CGG-specific IgH repertoires. CGG-specific IgH repertoires covering multiple D genes: IGHV9-3/IGHD3-1～IGHD4-1/IGHJ2. Heavy chain variable domain genes show that, CDR1 and CDR2 are encoded by V region; CDR3 is encoded by a part of V region and all of D and J regions.

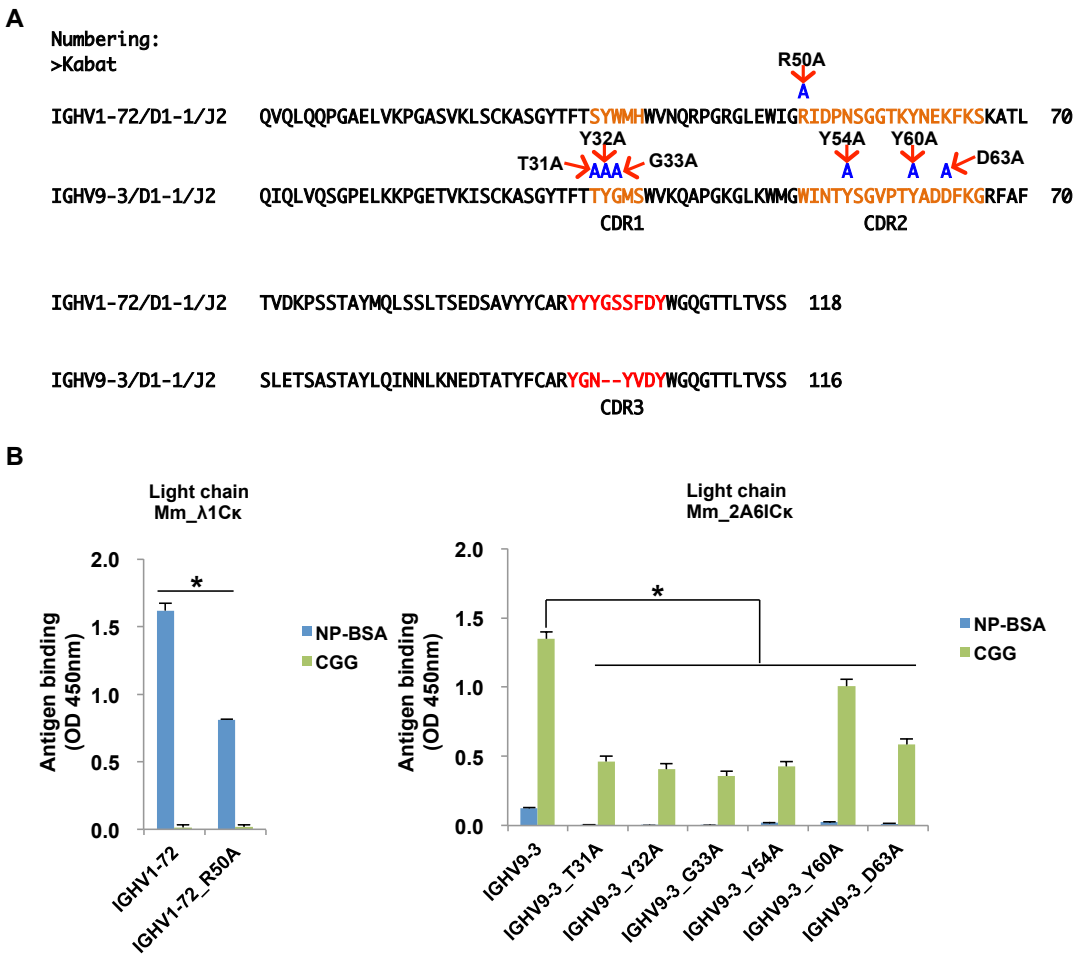

Fig. 16: The examination of the antigen-binding sites in IGHV1-72 and IGHV9-3. (A) The antibody numbering of IGHV1-72/D1-1/J2 and IGHV9-3/D1-1/J2 by Kabat scheme and the point mutations from the original amino acid to Alanine. CDR1 and CDR2 were annotated in orange; CDR3 was annotated in red. The mutations were labeled upon the originals in blue. (B) The binding capacities between the originals and mutations were tested by ELISA. The error bar indicates standard deviations of three independent experiments performed in triplicates. Statistical significance was tested using Student's *t*-test (*; $P<0.05$, $n = 3$).

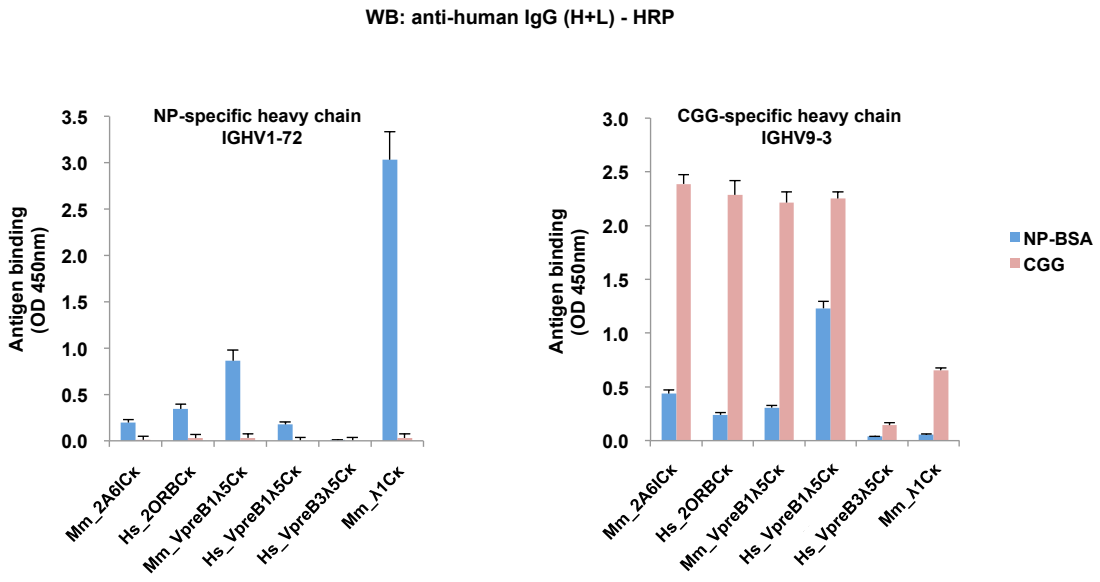

Fig. 17: Binding capacity of different antibodies to NP-BSA and CGG antigen. The supernatants were diluted in wash buffer, and the antibody concentration was adjusted to 10 µg/mL. Then, the samples were added to microtiter wells containing coated antigens at three different concentrations diluted from 20 µg/mL. The error bar indicates standard deviations of three independent experiments performed in triplicates. Statistical significance was tested using Student's *t*-test (*; $P<0.05$, $n = 3$).

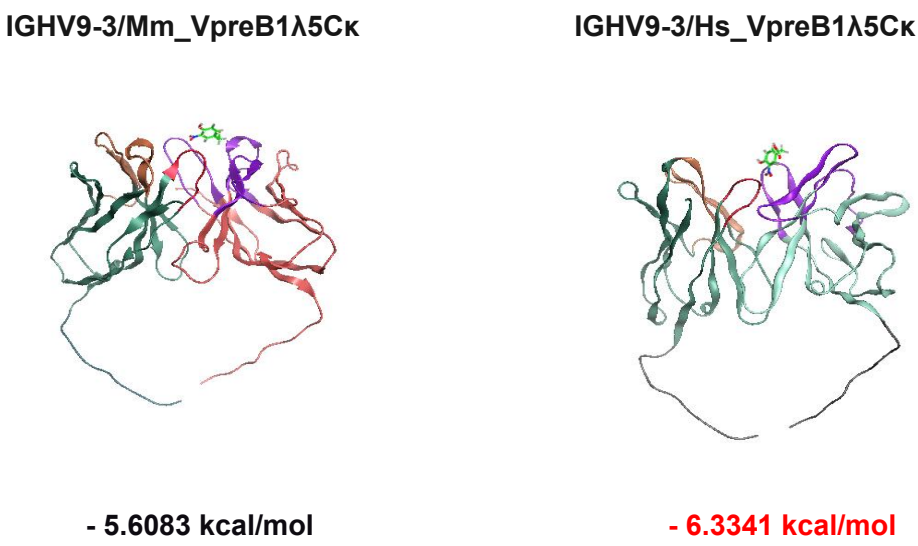

Fig. 18: *In silico* simulation for analyzing the non-specific binding to NPA in the antibodies containing IGHV9-3 and VpreB1λ5Cκ light chains. The docking results were shown as binding energy, suggesting that IGHV9-3 pairing with Hs_VpreB1λ5Cκ increased the non-specific of NP binding.

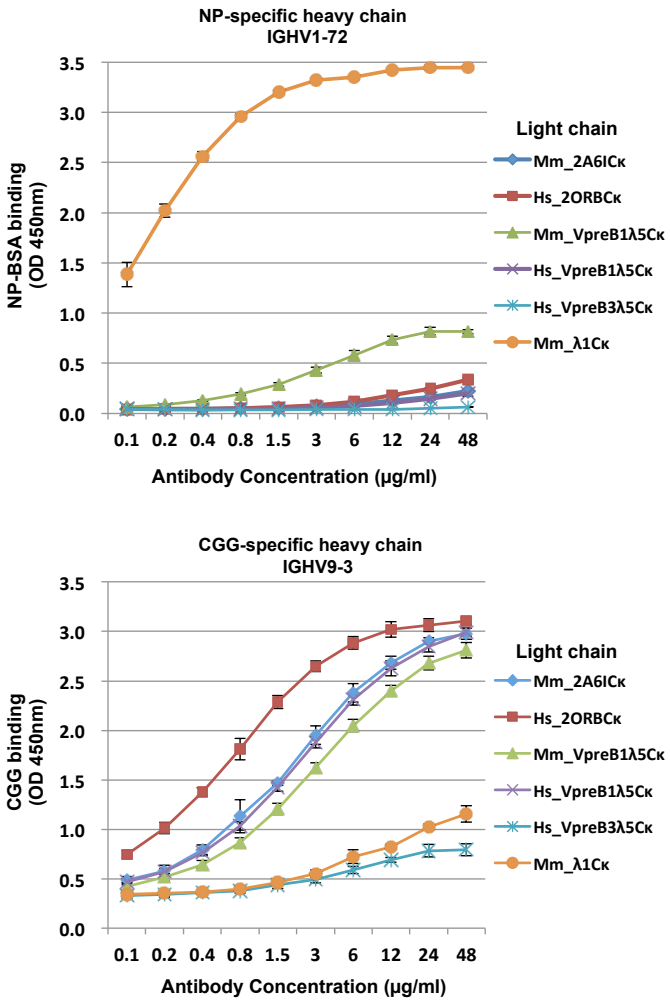

Fig. 19: Comparison of antigen binding affinity of different antibodies depending on the antibody concentration. The antigen concentration was diluted to 5 µg/mL. Antibody binding was detected with the goat anti-human IgG, (H+L) HRP conjugate. The binding activities of the antibodies are expressed in terms of O.D. 450 nm. Error bars indicate standard deviations of the means in three independent experiments performed in triplicates.

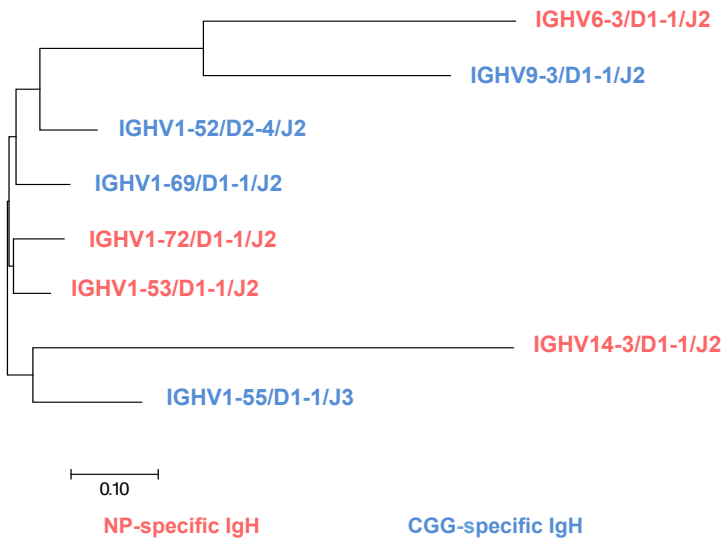

Fig. 20: Phylogenetic tree for antigen-specific IgH repertoires. The tree was generated using the neighbor-joining (NJ) algorithm with the MEGA7 software. Red, NP-specific; Blue, CGG-specific.

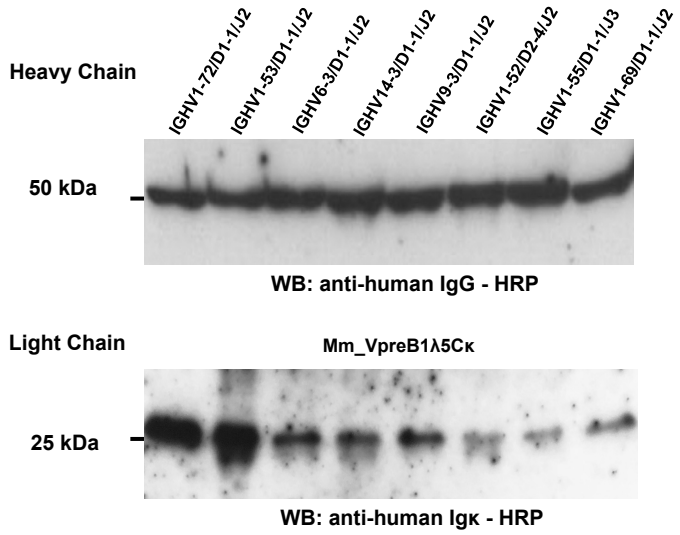

Fig. 21: Western blot analysis for the expression of recombinant antibodies. Equal volumes of cell culture supernatants were subjected to 12% SDS-PAGE, and antibody expression was detected with HRP-conjugated anti-human IgG antibody for heavy chains and HRP-conjugated anti-human Igκ antibody for light chains. Heavy chain bands are at the top, and light chain bands are at the bottom.

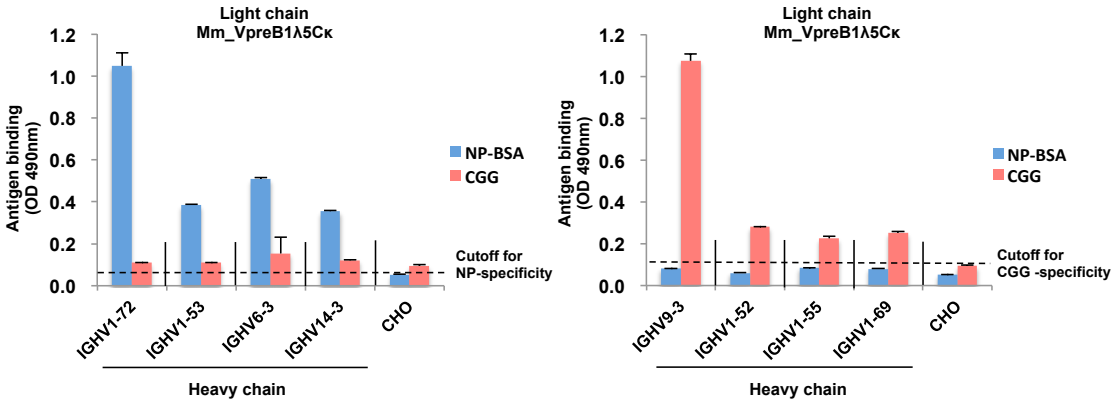

Fig. 22: Binding capacity of the recombinant antibodies to NP-BSA and CGG antigens. The cutoff was determined by the mean value plus standard deviation of CHO cell culture medium. The error bar indicates standard deviations of three independent experiments performed in triplicate.

A

PDB ID	Source	Antigen Tpye	Ligand	Antigen	Clan
1A3R	Mus Musculus	Protein	15 AA Human Rhinovirus Capsid Protein VP2	Human Rhinovirus	I
5EOQ	Mus Musculus	Protein	10 AA Protein A27 (Gene symbol: A27L)	Vaccinia virus	II
2HRP	Mus Musculus	Protein	10 AA Hiv-1 Protease Peptide	HIV	III

B

PDB ID	Source	Antigen Tpye	Ligand	Antigen	Clan
5ERW	Homo Sapiens	Protein	13 AA HCV E2 Glycoprotein Epitope II	HCV	I
3MOD	Homo Sapiens	Protein	11 AA Gp41 Mper-derived Peptide	HIV	II
4XMK	Homo Sapiens	Protein	11 AA Hiv-1 Jr-fl Gp120 V3 Peptide	HIV	III

Fig. 23: IgHs derived from different clans. Different IgHs were chosen as samples for testing the binding capacity, including the mouse-derived IgH sequences from the reported structures (PDB ID): 1A3R, 5EOQ and 2HRP; the human-derived IgH sequences from the reported structures (PDB ID): 5ERW, 3MOD and 4XMK.

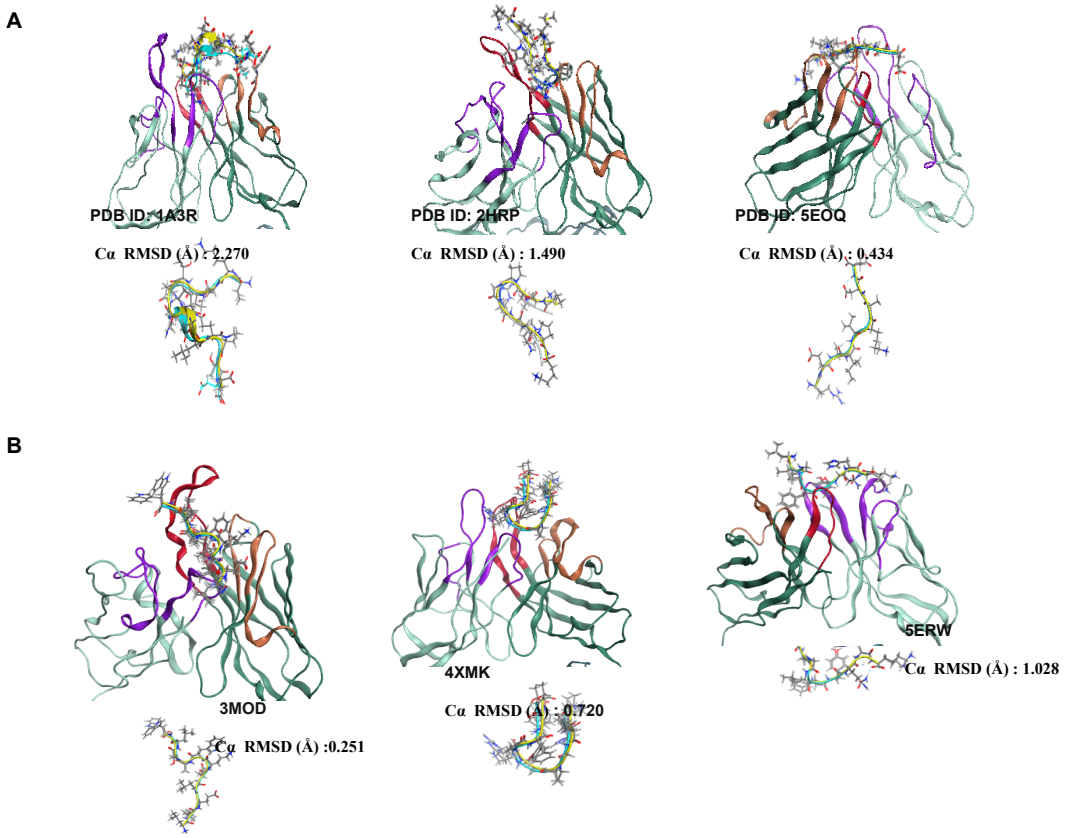

Fig. 24: Docking results of VpreB1λ5Cκ antibody structures (docked ligand: Yellow; co-crystallized ligand: Blue). (A) Mouse-derived IgHs pairing with Mm_VpreB1λ5Cκ. (B) Human-derived IgHs pairing with Hs_VpreB1λ5Cκ. The RMSD values between the co-crystallized and the docked ligands were shown.

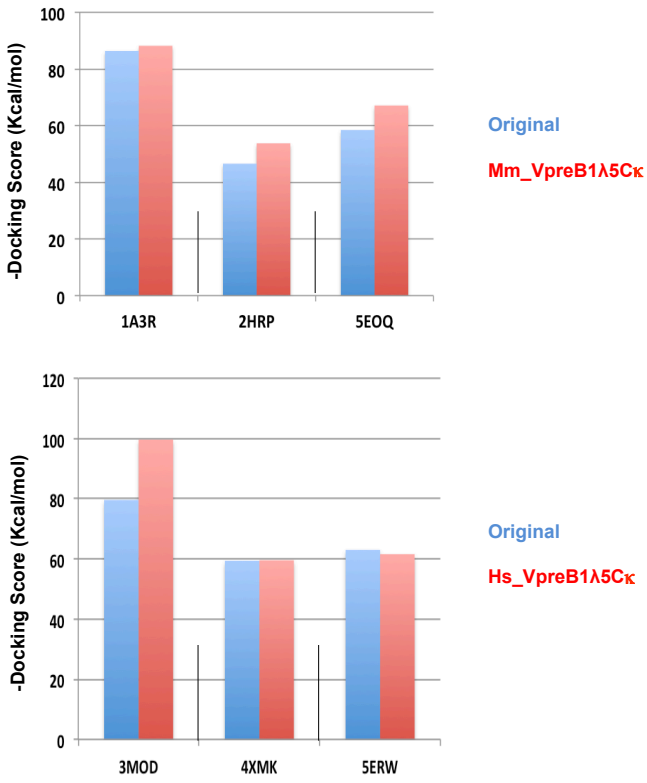

Fig. 25: The Plots for the binding energy after docking. The docking results of the original structures and VpreB1λ5Cκ structures are shown as - docking score (binding energy). The results of mouse-derived antibodies are on the top and those of human-derived antibodies are on the bottom.

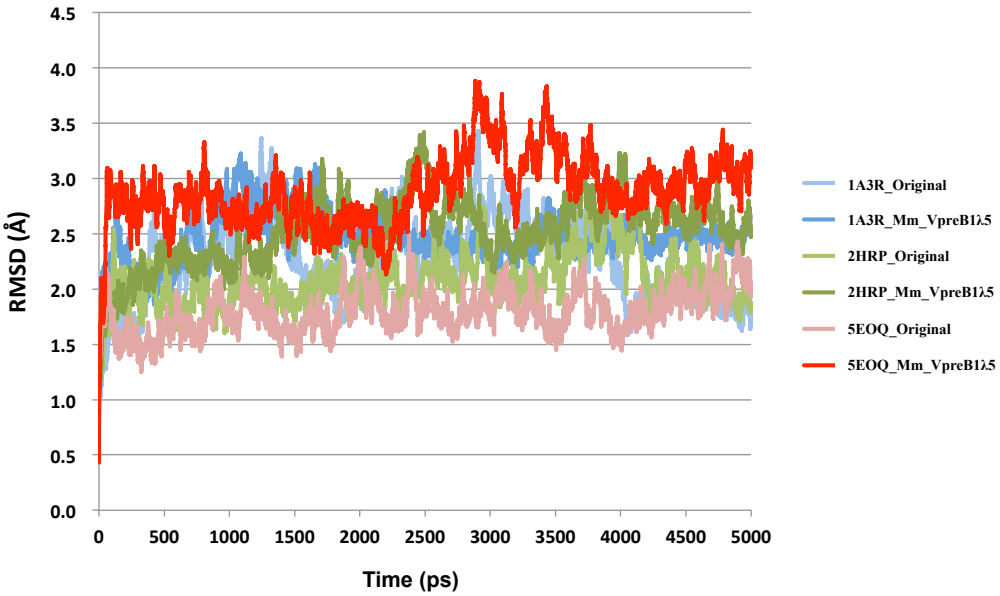

Fig. 26: The RMSD plots for MD simulations of mouse-derived antigen-antibody complexes. 5 ns molecular dynamics simulation were performed. The light colors indicate the original structures and the deep color indicate the Mm_VpreB1λ5Cκ structures.

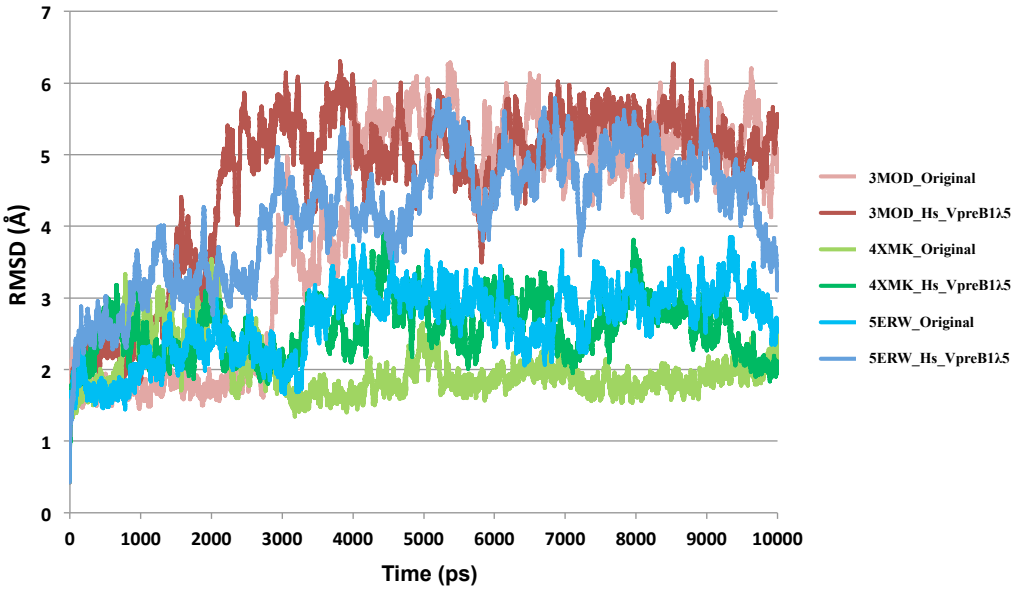

Fig. 27: The RMSD plots for MD simulations of human-derived antigen-antibody complexes. 10 ns molecular dynamics simulation were performed. The light colors indicate the original structures and the deep color indicate the Hs_VpreB1λ5Cκ structures.

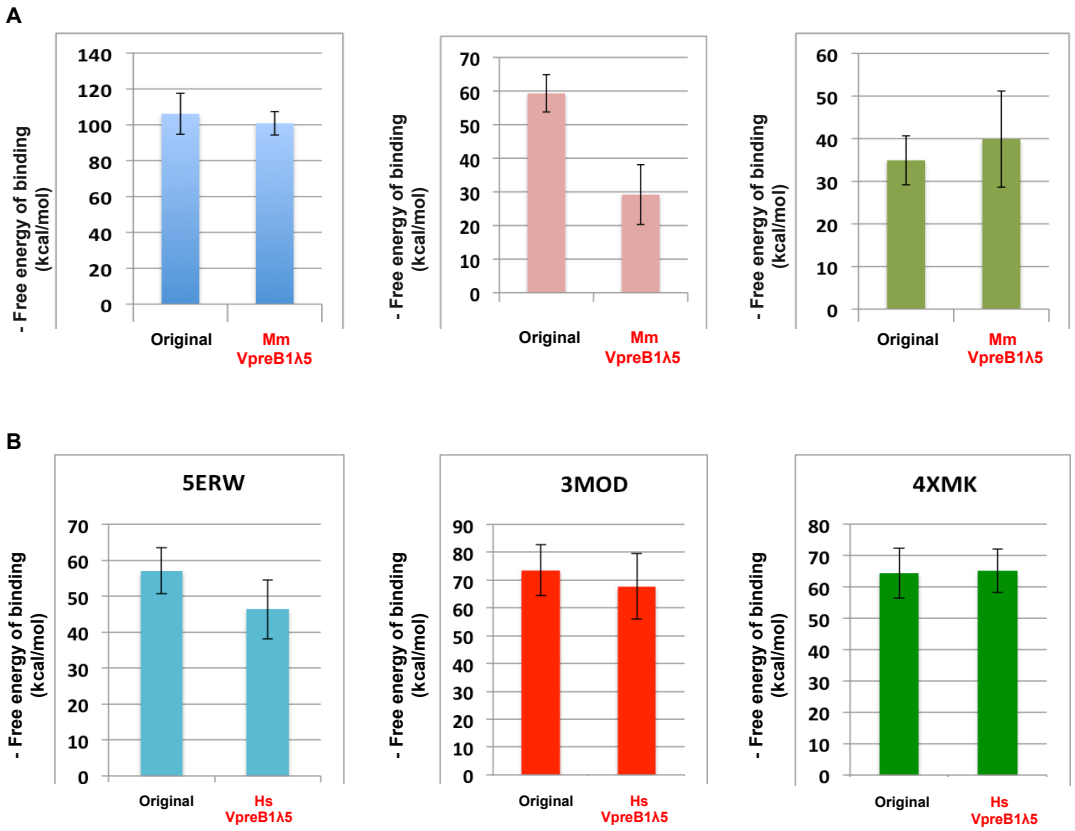

Fig. 28: Calculation of free energy of binding. The trajectories from the stable structures were chosen for the calculation of free energy of binding. The results of mouse-derived antibodies are shown on the top and the human-derived antibodies are shown on the bottom. The error bar indicates standard deviations.